Novel Insights for Smart Cell Search in Millimeter Wave Cellular Networks

By

Sana Habib

NUST201464075MSEECS61214F

Supervisor

Dr. Syed Ali Hassan

Department of Electrical Engineering

A thesis submitted in partial fulfillment of the requirements for the degree of Masters of Science in Electrical Engineering (MS EE)

In

School of Electrical Engineering and Computer Science,

National University of Sciences and Technology (NUST),

Islamabad, Pakistan.

(March 2017)

Approval

It is certified that the contents and form of the thesis entitled "**Novel Insights for Smart Cell Search in Millimeter Wave Cellular Networks**" submitted by **Sana Habib** have been found satisfactory for the requirement of the degree.

Advisor: **Dr. Syed Ali Hassan**

Signature: __________________

Date: __________________

Committee Member 1: **Dr. Sajid Saleem**

Signature: __________________

Date: __________________

Committee Member 2: **Dr. Fahd Ahmed Khan**

Signature: __________________

Date: __________________

Committee Member 3: **Dr. Rizwan Ahmed**

Signature: __________________

Date: __________________

Abstract

Millimeter wave (mmWave) technology is gaining momentum because of its ability to provide high data rates. However, in addition to other challenges in the operation of mmWave systems, developing cell search algorithms is a challenge due to high path loss, directional transmission, and excessive sensitivity to blockage at mmWave frequencies. Thus, the cell search schemes of long term evolution (LTE) cannot be used with mmWave networks. Exhaustive and iterative search algorithms have been proposed in literature for carrying out cell search in mmWave systems. The exhaustive search offers high probability of detection with high discovery delay while the iterative approach offers low probability of detection with low discovery delay. In this work, we propose a hybrid algorithm that combines the strengths of exhaustive and iterative methods. We compare the three algorithms in terms of misdetection probability and discovery delay and show that hybrid search is a smarter algorithm that achieves a desired balance between probability of detection performance and discovery delay.

Dedication

To Abu for inspiring me to always try to be the best in everything I do,

Ami for encouraging me to never loose ambition or drive,

Athar Mamu for guiding that the vision for the future should always diverge and never converge,

Taha, my light house, who always shows direction when I need one,

and

Nani, Maria & Phuppo for making the journey worthwhile.

Certificate of Originality

I hereby declare that this submission is my own work and to the best of my knowledge it contains no materials previously published or written by another person, nor material which to a substantial extent has been accepted for the award of any degree or diploma at NUST SEECS or at any other educational institute, except where due acknowledgement has been made in the thesis. Any contribution made to the research by others, with whom I have worked at NUST SEECS or elsewhere, is explicitly acknowledged in the thesis.

I also declare that the intellectual content of this thesis is the product of my own work, except for the assistance from others in the project's design and conception or in style, presentation and linguistics which has been acknowledged.

Author Name: **Sana Habib**

Signature: ________________

Acknowledgment

I am grateful to my university for creating an atmosphere that is conducive to learning and providing various opportunities for professional and academic growth via conferences, lectures by distinguished leaders/researchers, and events (like IEEE WIE).

I wish to express my deepest gratitude to Dr. Syed Ali Hassan for his guidance, support, useful insights and reviews on my draft and simulation environment that helped in significantly improving the work. In particular, the show down of knowledge and bombardment of ideas during my weekly meetings has been a great source of motivation.

Next, I am greatly thankful to Dr. Ali Arshad Nasir, for his availability and patience in reviewing the drafts that I wrote while working on the thesis. His comments and suggestions have been very helpful in shaping the direction of research. I am also grateful to Dr. Hani Mehrpouyan for taking out the time to provide useful feedback on my work.

Next, I wish to thank Hamnah, Soma, and Aneeqa for always being there to help me with the nitty gritty details related to my work. A special thanks to the highly energetic undergraduate students: Akber, Amna, Atif, Zain, Shahzeb, Rida, Rushda, Osama, and Usman for creating the most friendly and lively environment in Information Processing and Technology (IPT) Lab. Their excitement and discussions about the upcoming scholarships and future excited and inspired me a lot.

Table of Contents

List of Figures

List of Tables

Chapter 1

Introduction and Motivation

“There’s a difference between the way we approach 5G spectrum and the rest of the world. We will allocate 5G spectrum faster than any other nation on the planet. We then will get out of the way and let innovation and competition reign.” — Tom Wheeler (Chairman FCC)

1.1 Motivation

The fourth generation (4G) of mobile communication has been a tremendous breakthrough in cellular industry. With the proliferation of smart phones, tablets, and ever increasing number of devices that are connected to the Internet, data rate demands continue to rise. Furthermore, interesting new applications that go beyond personal communications are further anticipated to increase the number of portable devices to tens or hundreds of billions [28, 44, 53]. With the deployment and maturity of 4G, researchers are now

Figure 1.1: The Future with 5G

beginning to ponder over the question of what's next [17]?

This curiosity has led to the dawn of fifth generation (5G) of mobile communication. 5G is not just an incremental advancement on 4G but a quantum leap as it is capable of providing massive amounts of bandwidth, very high download speeds, and unmatched antenna gains [15]. In comparison to mega bit download speeds of 4G, 5G provides data rates on the order of giga bits per second (Gbps). By the virtue of the annual visual network index (VNI) report, released by Cisco, we now have a timeline of 2020 by which the vision of 5G will become a reality [27].

5G is timely and capable of reinforcing the concepts of cloud computing [72, 92], resource pooling [90], software defined networking [36, 78], and network function virtualization [25,35], etc. The most interesting application bolstered by 5G is Internet of Things (IoT) [91], which is a concept whereby anything and everything will be on the Internet. Interestingly enough, there will be a point in time when more things are connected to the Internet than

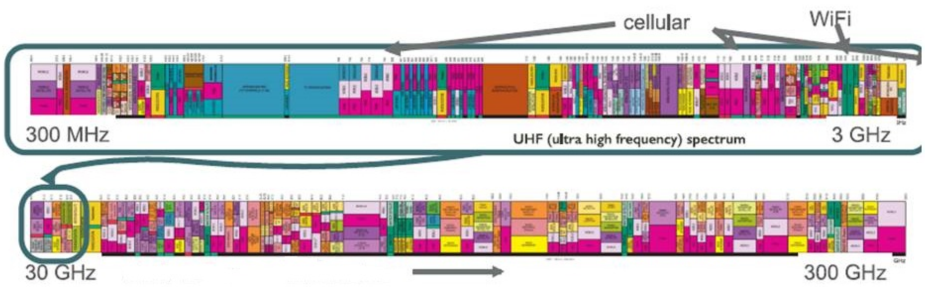

Figure 1.2: FCC Spectrum Chart [54]

people. Moreover, 5G is envisioned to make self driving cars capable of time critical decisions and providing virtual reality experience.

Imagine how fascinating it would be if students do not need to bring back pack to the university; instead they could stand under a 5G access point and download whole books. 5G is the key enabler for this concept of *information shower*, whereby high speed access points mounted on roadways, sidewalks, universities will be able to provide all the necessary information in seconds. Because of providing high download speeds, 5G will significantly enhance user's quality of experience (QoE), e.g, heavy movies like Captain America can be downloaded in seconds using 5G rather than minutes with 4G.

This huge excitement in the world of 5G boils down to the simplest question of how to achieve the high data rate and bandwidth goals? To answer this question, we refer the reader to Fig. 1.2, which shows two slices from the United States Federal Communications Commission (FCC) spectrum chart. The upper slice shows low frequency spectrum and the lower slice contains high carrier frequencies. The current legacy systems utilize the upper slice, i.e., the low frequency spectrum from 3 GHz – 30 GHz. This band of frequencies that is allocated to military, cellular service provides, etc, is crowded and does not has any more capacity. The brilliant idea of moving up in the frequency spectrum, i.e., using the band from 30 GHz – 300 GHz, in order to have channels that can provide much higher data rates and bandwidth is the foundation for 5G communication and the corresponding band of carrier frequencies is called *millimeter wave (mmWave)* frequency band [23, 31, 38, 56, 58, 59, 69].

Note that this intriguing concept of mmWave frequency band is not new but as old as wireless communication itself. In fact, J.C. Bose, in 1895 at Calcutta, India, carried out his research using frequencies as high as 60 GHz. He later presented his research at Royal Institution, London in 1898. Lebedew, (around the same time) in Russia, also demonstrated results using high carrier frequencies that are classified today as mmWave spectrum. Realizing the tremendous potential of mmWaves for future communications, Theodore. S. Rapport stated:

> *This is probably the biggest thing that has happened to the wireless industry in the last* 20 *years since Qualcomm shook the world with the idea of code division multiple access (CDMA), moving the processing from RF filters of the old analog phones down to base band where silicon and chips could do the processing. MmWave technology is just that fundamental, where the wavelengths are as small as a finger nail, allowing new antennas to go on a portable device.....thousands of antennas on a base station (BS) and hundreds of antennas on the portable device. This is a completely new approach to wireless communication; brand new theories, brand*

new techniques, new standards, propagation laws, channel models, standardization techniques, all are wide open. It is really the dawn of an entire new age.

1.2 Contribution

MmWave technology is a relatively recent field. The bulk of information that exists on mmWave systems need to be organized and categorized in order to provide a manageable overview of the state-of-the-art. In particular, initial access with mmWave systems is a challenge due to their peculiar characteristics of high frequency/short wavelength, high path loss, directivity, and sensitivity to obstacles, which makes this area ripe for research and novel ideas/new algorithms are particularly welcomed by the researchers in the field. Understanding that, we make the following specific contributions:

1. We summarize and overview the key characteristics of mmWave systems that distinguish them from legacy systems and run through the recent research in the area of initial access with mmWave technology (Chap. 2, Chap. 3).

2. Going deep in the area of initial access, we develop a mathematical framework in order to study the existing cell search solutions. Using that theoretical framework, we enhance the existing study by proposing a new algorithm called *hybrid* search, which is based on the idea of combining the strengths of the two well-established schemes (i.e., exhaustive and iterative) in the cell search literature (Chap. 4).

3. We perform a comparative analysis by analyzing the misdetection probability and discovery delay of the three cell search algorithms along four aspects: signal-to-noise-ratio (SNR), separation distance between base station and user equipment, user orientation with respect to the base station, and search beamwidth (Chap. 5).

4. Towards the end, we identify the open research questions and challenges in order to provide directions for future research Chap. 6).

The concept of unleashing the bandwidth by moving up in the frequency spectrum has attracted considerable attention from the research community. Specifically, two notable research groups led by Robert W. Heath (at University of Texas, Austin) [3] and Theodore S. Rappaport (at New York University) [2] are actively working in this area.

With the realization of the great impact that mmWave technology has for 5G, researchers and practitioners are relentlessly working in the field and there is a need for a strong work that could benefit communication system engineers. Our work is timely due to the emerging new trends and research in this domain and successful small scale real world deployment/testing of mmWave systems. The objective of this work is to benefit the communication community by organizing the existing literature on initial access for mmWave systems and presenting a *hybrid* cell search scheme that achieves a balanced trade-off between detection probability and discovery delay.

Chapter 2

Hallmarks of mmWave Systems

> **"Over the last 40 years, computer clock speeds and memory sizes rose by as much as six orders of magnitude. Yet communications frequencies have barely moved. The only hope to meet mobile traffic demand is to utilize more spectrum." — Theodore S. Rappaport (Director of Wireless Research Group at New York University)**

Being an influential technology, several standardization efforts for mmWave wireless personal area networks (WPAN)/wireless local area networks (WLAN) are underway, such as ECMA-387 [8, 70], IEEE 802.15.3c [4], and IEEE 802.11ad [6]. The key frequency bands in mmWave spectrum, which have attracted considerable attention from the research community because of their favorable propagation characteritics are 28–30 GHz (also known as the local multi-point distribution service), 60 GHz (license free band), and E-band that includes 71–76 GHz, 81–86 GHz, and 92–95 GHz [23].

MmWave systems have some peculiar characteristics of high path loss, directivity, and sensitivity to blockage by humans as well as obstacles. These attributes make communication with mmWave systems a challenge. Nevertheless, persistent efforts by the researchers in the field has debunked the myth that communication at higher frequencies is not possible [55, 71, 86]. In this chapter, we give a gist of these design challenges and dig deep into the range, propagation laws, and channel measurements for mmWave systems.

2.1 High Path Loss

MmWave systems operate at very high carrier frequencies, due to which they experience high path loss in comparison to traditional cellular systems that operate at low frequencies. By Friis equation [65], the free space propagation loss ($FSPL$) is proportional to the square of carrier frequency f:

$$FSPL = (4 * \pi * R * f)^2 \tag{2.1}$$

where R is the radial distance between transmit and receive antennas. To give an idea on the additional path loss experienced at high frequencies, we recommend the use of Eq. 2.1 to calculate that the path loss beared at 28 GHz, 38 GHz, 60 GHz, and 73 GHz is approximately 11, 15, 24, and 29 decibels (dB) more than that at 2.5 GHz. In addition to that, a serious concern associated with using high carrier frequencies for communication is that they experience high rain attenuation, atmospheric, and molecular absorption losses [1, 45, 61].

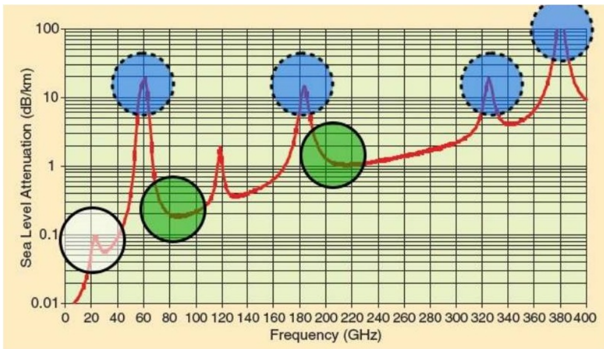

Figure 2.1: Sea level attenuation vs Frequency [75].

We refer the reader to Fig. 2.1 that shows attenuation for different operating frequencies. The white circle in Fig. 2.1 show the frequency bands that experience low attenuation. In particular, these frequency bands (i.e., 28 GHz and 38 GHz) are considered suitable for future 5G communications.[1] The green circles mark the frequency bands (e.g., 73 GHz) whose free space propagation characteristics are comparable to modern cellular frequencies while blue circle shows frequencies with greater attenuation (e.g., 60 GHz) that are suitable only for short range indoor communications. Note that rain attenuation and oxygen absorption losses are more significant in the 60 GHz and 73 GHz bands as compared to the 28 GHz and 38 GHz bands [56].

This challenge of high isotropic path loss is not insurmountable as mmWaves facilitate small antenna sizes and thereby the use of large antenna arrays. The high beamforming gains achieved by using directional transmission compensates for high path loss. The directional transmission between a base station (BS) and a user equipment (UE) is shown graphically in Fig. 2.2. With

[1] Zhao and Li [61] studied the effect of rain attenuation at these frequencies by considering a very heavy rainfall of 25mm/hour and found out that rain attenuation is only 1.4 dB at 28 GHz and 1.6 dB at 38 GHz, thereby implying that rain attenuation could be compensated for by proper link design in future mmWave cellular systems.

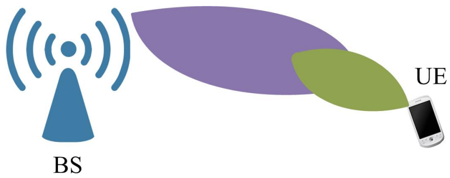

Figure 2.2: Directional Transmission.

small cell sizes (on the order of 200m) becoming the norm in order to improve spectral efficiency, rain attenuation, atmospheric, and molecular absorption losses do not cause any significant additional path loss and channel measurements in real world environments have ensured the feasibility of high carrier frequencies for future wireless systems [16, 18, 52, 66, 69, 75, 83, 93].

Due to high attenuation losses, the license free band at 60 GHz contains no significant multipath component and relies on line of sight (LoS) transmission for communication [14,21,30,37,68,82,88,95]. To elaborate, consider the line of sight (LoS) channel model proposed in 802.11ad for indoor environments at 60 GHz [6], which shows that direct path contains maximum energy and can simply be regarded as additive white gaussian noise (AWGN) channel while the non line of sight (NLoS) channel model contains no direct path and the number of paths with considerable amount of energy is small.

On the other hand, the channel measurements at 28 GHz, 38 GHz, and 73 GHz show strong signal reception even in NLoS channel conditions from cell sites that are in the range of 100 - 200 m [16,18,52,66,69,75,83,93]. We further refer the reader to [56] in order to have a look at the path loss exponent measurements for LoS and NLoS channels at a specific operating frequency using fixed antenna gain and a particular beamwidth. Having discussed the path loss and channel characteristics, we next move on to discussing directional transmission.

2.2 Directivity

The high path loss of mmWaves is compensated using directional transmissions [73,84]. Due to the advances in complementary-metal-oxide-semiconductor (CMOS) technology, large electrically steerable antenna arrays that are capable of providing high beamforming gains and consequently magnitudes of increase in capacity are possible [32, 42, 68]. In order to steer a beam in a desired direction, the phase of the signal transmitted by each antenna element present on large antenna arrays that are realized as metal patterns on circuit board is controlled such that the directed beam contains aggregated signal power [10, 42, 49, 50]. This scheme is referred to as *beamforming*.

This way, using beamforming, the high path loss is compensated without the need to increase transmit power. Note that beamforming gain is high in the desired direction and negligible in other directions. In order to make the transmitter and receiver direct their beams towards each other, beam training is needed and many beam training algorithms that reduce beam alignment time have been proposed in literature [60, 85, 89]. In comparison to the beamfoming used with microwaves (μ-Waves), mmWaves enable much narrower search beams that offer high gains. This feature is shown pictorially in Fig. 2.2.

The three physical architectures used for realizing beamforming are: digital beamforming, analog beamforming, and hybrid beamforming. Digital beamforming allows the creation of multiple beams and sending them simul-

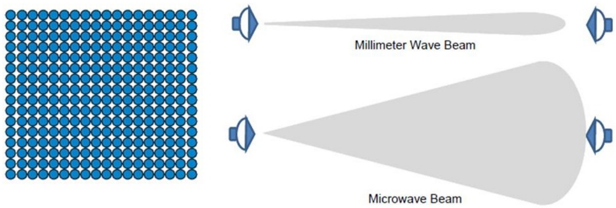

Figure 2.3: Antenna array (left) and mmWaves vs μ-Waves search beam (right) [5].

taneously in multiple directions, thereby reducing discovery time but at the expense of high power consumption and costly architecture. This high power and cost is associated with the number of antennas/baseband to RF chains[2] (as digital beamforming uses an RF chain per antenna element). Analog beamforming, on the other hand, uses one beam/baseband to RF chain per time slot for searching [87]. It is less complex, consumes less power but can delay discovery process. Hybrid beamforming achieves a good balance between analog and digital beamforming by using a large number of antennas with limited number of RF chains [43]. Note that these beamforming architectures and the appropriateness of a particular architecture for use in a certain scenario are the design issues related to physical layer. We reviewed these schemes purely for the purpose of self-containment and have summarized the hardware complexity, power requirements, and search time for each of the three schemes in Table 2.1.

[2]RF chain includes analog to digital and digital to analog converters, power amplifier, mixers, upconverters, etc

Table 2.1: Comparison Between BF architectures

Architecture	***Hardware complexity***	***Power Requirements***	***Search Time***
Analog	Low	Low	High
Digital	High	High	Low
Hybrid	Reasonable	Reasonable	Reasonable

2.3 Sensitivity to Blockage

MmWaves, due to operating at very high carrier frequencies have extremely small wavelength. For example, the wavelengths at 28 GHz, 38 GHz, 60 GHz, and 73 GHz are approximately 11mm, 8mm, 5mm, and 4mm respectively. Electromagnetic waves have weak ability to diffract around objects whose size is considerably larger than the wavelength. Thus, mmWave systems are highly sensitive to blockage by humans as well as obstacles.

In particular, the human body can attenuate mmWave signals by as much as 35 dB [51,64]. Objects like brick and glass can cause an attenuation around 80 dB and 50 dB respectively [11, 13, 69, 93]. Human mobility, which is high in indoor environments, can introduce significant intermittency in mmWave links and relay nodes may be used in order to ensure reliability [82].

In addition to that, *deafness* is also a blockage problem that occurs when main beams of transmitter and receiver do not point towards each other, thereby preventing the establishment of a communication link [26, 79]. Deafness simultaneously provides the benefit of reducing interference as well as the detriment of complicating link establishment phase [81]. Hence, in mmWave systems, we move from the *interference limited* to the *noise limited* regime,

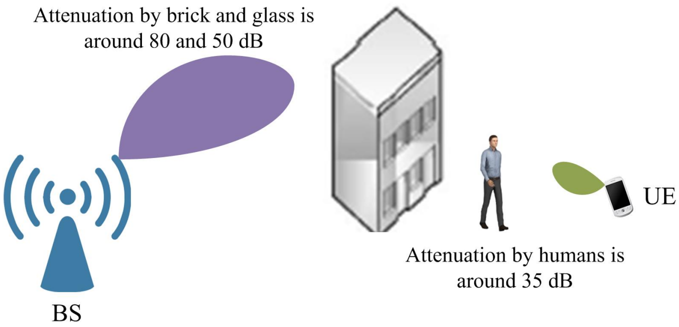

Figure 2.4: Sensitivity to Blockage

which significantly affects coordination mechanisms such as initial access, resource allocation, to name a few.

If the communication path between the transmitter and receiver gets blocked due to stationary or moving humans and objects, then an alternate communication path needs to be searched. With the result, beamforming overhead, discovery delay, etc will be elevated. Thus, due to randomly located objects, the traditional notion of cell boundary needs to be redefined with mmWaves. Consequently, researchers are moving towards the paradigm of *dynamic cell*; whereby cell boundries are dynamically remodeled to meet quality of service (QoS) requirements in applications such as high definition television (HDTV) and overcome blockage.

Due to sensitivity to blockage, mmWave channels are sparser than classical cellular systems. In order to provide better coverage, the idea of heterogeneous networks (HetNets) is gaining attention whereby both mmWave and μ-Waves BS operate in combination. This can compensate for the intermittency in mmWave links due to blockage [94]. Thus, mmWaves could be deployed in two modes depending on the geographical constraints of the environment: stand-alone mode (i.e., a complete mmWave network) and integrated networks (i.e., containing both mmWave and μ-Wave systems).

High path loss and directionality in combination with blockage and deafness makes coordination mechanism in mmWave systems a key design concern. Coordination mechanisms typically include synchronization, initial access, resource allocation, interference management, handovers, etc [79]. These issues are typically dealt with at the medium access control (MAC) layer and need to be modified in order to become suitable for use with mmWave systems [33, 34]. For the purpose of our study, we focus only on initial access in the next chapter. However, the interested reader is referred to [79] for a more thorough study.

Chapter 3

Initial Access: Opportunity or Challenge?

> **"The real motivation for thinking about using millimeter wave carrier frequencies instead of lower frequencies is just that there is the potential to have channels with much.... much larger bandwidths." — Robert W. Heath (Professor at University of Texas, Austin)**

Initial Access (IA) is a process by which a base station (BS) and user equipment (UE) establish a physical connection with each other, after which the formal communication starts. The process of IA consists of three steps: cell search, extraction of system information, and random access. Cell search is the method during which UE searches for the BS and associates with the one from which it receives the strongest signal. Once the connection has been established, the BS and UE exchange important system information such as cell configurations, downlink and uplink bandwidth, frequency band, number of transmit antennas, cell identity, etc in a process called extraction of system information. UE, having searched for an appropriate BS and extracted system information, next obtains a channel for communicating with the BS by sending channel reservation request to BS using contention-based or contention-free protocols, a scheme referred to as *random access*. At the conclusion of IA process, the user is connected to the data plane and able to transmit/receive actual data. The process of IA gets complicated with mmWave systems due to their hallmarks of high path loss, directional transmission, and sensitivity to obstacles.

In this chapter, we overview the current state of the art with IA. In particular, our discussion revolves around two topics. We first discuss the IA procedure of long term evolution (LTE), as it can be considered a technological predecessor for mmWave systems and provides the necessary foundation based on which IA for mmWave technology can be designed. Then we move towards discussing the design of synchronization signal that is used with LTE. The process of aligning beams between the transmitter and receiver takes time. In order to improve this beam alignment time, several efficient beamforming algorithms and detector design have been proposed in literature that we briefly discuss.

3.1 Related Work

The current cellular systems such as long term evolution (LTE) have support for beamforming and multi-antenna technologies [77]. LTE carries out cell search using a two step synchronization procedure. First, the LTE BS omni-

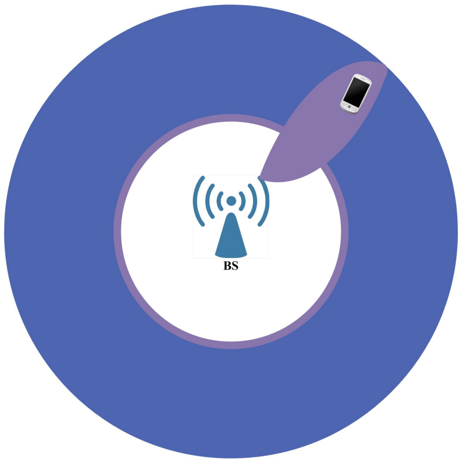

Figure 3.1: Range Mismatch Problem [20].

directionally transmits pilot signals (without exploiting beamforming); once a link with the UE has been established, formal communication takes place using directional transmission. With mmWaves, it is important to exploit antenna gain even during cell search. Otherwise, the high antenna gains would create a disparity between the range at which a cell can be detected (before beamforming directions are known and the antenna gain is not available) and the range at which reasonable data rates can be achieved using beamforming. This problem is referred to as range mismatch problem or asymmetry in gain problem [48, 67]. The range mismatch problem is shown graphically in Fig. 3.1, whereby white circle marks the range that can be covered using omnidirectional transmission and blue circle identifies the range with directional transmission. If cell search does not exploit antenna gain then mobiles outside the white circle may go undetected despite being capable of high data rates. This means that IA process of LTE, despite providing a good foundation can not be used for mmWave systems. Having said that, the synchronization signal design of LTE provides the necessary ground work

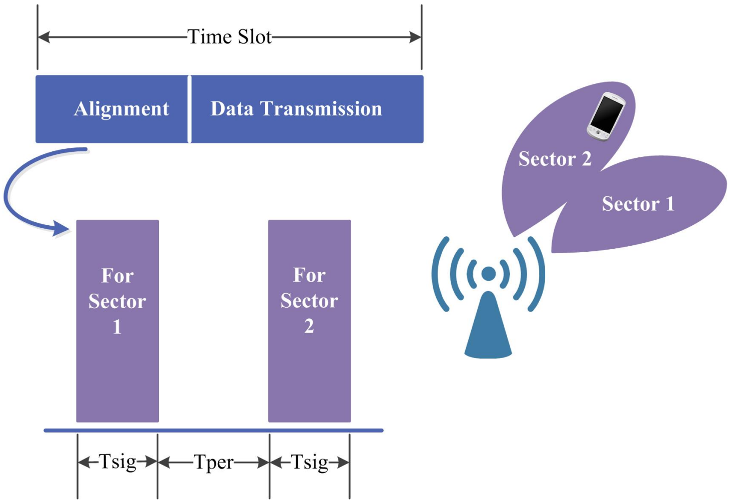

Figure 3.2: Synchronization Signal and Initial Access.

for mmWave synchronization signal design and is the topic of discussion in the next subsection.

3.1.1 Synchronization Signal

In the LTE standard, each BS (known as the evolved NodeB or eNB) periodically transmits two signals: the Primary Synchronization Signal (PSS) and the Secondary Synchronization Signal (SSS) [29]. The UE searches for the BS by scanning various frequency bands for the presence of these signals. The UE first searches for the PSS that provides a coarse estimate of received power. For simplification, there are only three PSS signals and one of them is transmitted. After the detection of PSS, UE searches for SSS. The SSS can belong to a larger set of 168 waveforms. The detected index of PSS and SSS waveforms together convey the eNB cell identity. As there are 3 PSS signals and 168 SSS signal, upto $(168)(3) = 504$ cell identities can be communicated with the two signal indices. After detecting an eNB through the cell search, next steps of extraction of system information and random access process occur to conclude IA.

To understand the dynamics of synchronization signal, we refer the reader to Fig. 3.2. The figure shows the structure of a time slot, which contains two parts. The first part is for beam alignment and the second for data transmission. Beam alignment is a process that can take time depending on the particular cell search algorithm used. Once the beams of BS and UE have been aligned, then data can be transferred. As seen from Fig. 3.2, during the beam alignment phase, the synchronization signal is transmitted periodically with a period T_{per} for T_{sig} s. Depending on the particular beamwidth used, T_{sig} is transmitted in each sector and the search process stops once the beams between transmitter and receiver are aligned. Since it takes time to learn direction between BS and UE, we next summarize some important directional beamforming techniques. Note that the focus of our study is on cell search, the direction beamforming literature has been over-viewed to make the thesis self-contained.

3.1.2 Directional Beamforming

For directional beamforming, the well established direction learning methods in signal processing literature, such as MUltiple Signal Classification (MUSIC) and Estimation of Signal Parameters via Rotational Invariance Techniques (ESPRIT), offer increased complexity in the mmWave regime [47, 74, 76]. Realizing the need for low complexity beamforming approaches, Raghavan et al. [62,63] studied initial UE discovery in mmWave systems and proposed the structure of an optimal beamformer with per-antenna gain and phase control.

The alignment between transmitter and receiver is a time consuming process, and this trade-off is widely known in literature as alignment-throughput trade-off. To elaborate, a wider beam reduces alignment overhead but also provides reduced directivity gains. Furthermore, existing mmWave standards schedule only one transmission per time slot. Shokri-Ghadikolaei et al. [80] proposed two standard-compliant approximation algorithms (that rely on underestimation and overestimation of interference), which maximize spectral reuse while providing constraints on the directionality level and number of concurrent transmissions that could be pursued. A key result found by their research is the fact that narrow beams in-general are not optimal.

Abu-Shaban et al. [7] examined two beamforming schemes, random-phase beamforming (RPBF) and directional beamforming (DBF) and showed by simulation results that RPBF is more appropriate as it attains a lower cramer rao bound (CRB) with fewer beams in comparison to DBF. Barati et al. [19, 20] studied the issue of directional cell search with mmWave systems along three design questions; first, how mmWave UE keeps track of direction of arrival of synchronization signal from BS, second, whether omnidirectional or randomly varying directional search is a better option for the mmWave BS, and the effect of using analog or digital beamforming at the UE. Their two key findings are that digital beamforming outperforms analog beamforming and omnidirectional transmission outperforms random directional scanning. We further refer the reader to [62, 63], for a thorough understanding on the efficacy of different beamforming approaches for initial UE discovery in mmWave systems.

Having laid some foundation on the design challenges and the current literature that exists on IA, we now move towards the main objective of this dissertation, i.e., cell search with mmWave systems.

Chapter 4

Withstanding the Obstacles: Cell Search Schemes

> **"Coming together is a beginning; keeping together is progress; working together is success."— Henry Ford**

The IA process of LTE can not be used with mmWave systems due to range mismatch problem and additional sensitivity to blockage. Realizing the need for new cell search schemes, researchers have proposed three key algorithms, i.e., exhaustive, iterative, and context-information (CI) based cell search that cater for range mismatch problem and sensitivity to blockage [39]. While studying these algorithms, detection probability and discovery delay are the two key parameters that need to be taken into account. Note that the focus of this dissertation is only on downlink transmission. As CI-based search scheme uses exhaustive search in downlink, so we do not go into its details as results from exhaustive search can simply be extended to it. Interested reader is however referred to [24, 41].

It is important to mention the noticeable work of Giordani et al. [39] that served as a foundation for our work. Nevertheless, their work lacks a mathematical foundation for deeply investigating the algorithms. We enhance the existing study by first quantifying the already proposed cell search schemes (i.e., exhaustive and iterative). The mathematical framework developed for this purpose serves as the building block for hybrid algorithm, which achieves a desirable balance between detection probability and discovery delay. In addition to that, this is the first work to also consider the effect of UE orientation on discovery delay; a parameter that has not been explored in detail before.

The first well established cell search algorithm proposed in literature, namely, exhaustive search provides a very good detection probability but takes a longer duration to discover the UE in comparison to iterative search approach [39,46]. Iterative search [12], because of iteratively narrowing down search beams outperforms exhaustive search in terms of discovery delay but has a low detection probability. Thus, there is an inevitable trade-off between these two algorithms. We can either achieve high detection probability and high discovery delay (exhaustive search) or low detection probability and low discovery delay (iterative search). A desirable balance between detection probability and discovery delay is indeed possible and is the main contribution of this dissertation. We will go into its details in section 4.3, but first we discuss the well established cell search algorithms in literature.

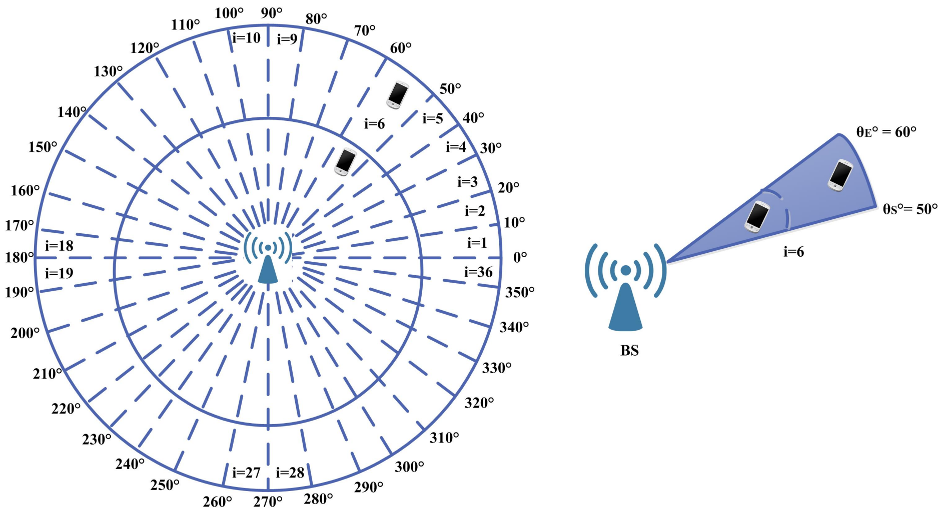

Figure 4.1: Exhaustive Search.

4.1 Exhaustive Search

In this method, the BS starts its search for UE by transmitting the synchronization signal, T_{syn}, with a search beamwidth BW°_{EX}, for T_{sig} seconds (s) in a particular sector. Let N_{EX} be a positive integer that denotes the total number of search sectors, then we have

$$N_{EX} = \frac{360^{\circ}}{BW^{\circ}_{EX}} \tag{4.1}$$

For example, if $BW^{\circ}_{EX} = 10^{\circ}$, then $N_{EX} = 36$. These 36 search sectors using $BW^{\circ}_{EX} = 10^{\circ}$ are shown in Fig. 4.1 (left). Let $I = \{1, 2, ...N_{EX}\}$ is a set that represents the index of sectors. Note that we have assumed sectored approximation, i.e., the gain provided by search beam is constant throughout the sector $i \in I$ as shown in Fig. 4.1 (right). The search region spanned by the beam for a particular $i \in I$ is found as

$$
\begin{aligned}
\theta_S^\circ &= (i-1)BW_{EX}^\circ, \\
\theta_E^\circ &= (i)BW_{EX}^\circ,
\end{aligned}
\tag{4.2}
$$

where θ_S° marks the start of the beam and θ_E° identifies the end of a beam. Hence, in the above example, for $i = 1$, the search beam spans the region, 0° to 10°.

If $G(\theta)$ is the total antenna gain, then

$$G(\theta) = G_{Tx} + G_{Rx} + BFGain_{Tx} + BFGain_{Rx}, \tag{4.3}$$

where G_{Tx} and G_{Rx} are the antenna gains due to omnidirectional transmission at the transmitter and receiver, respectively, while $BFGain_{Tx}$ and $BFGain_{Rx}$ are gains due to beamforming at the transmitter and receiver, respectively. $BFGain$ at either the BS or UE is defined as

$$BFGain = E * D, \tag{4.4}$$

where E is the antenna efficiency and the directivity, D is given as

$$D = \frac{4\pi}{BW^\circ}, \tag{4.5}$$

Now, T_{syn} passes through a channel that can be line-of-sight (LoS) or non-line-of-sight (NLoS). Let the path loss experienced by the signal be

$$L_{mm}(r) = \begin{cases} \rho + 10\alpha_L log(r) + \chi_L & \text{if link is LoS} \\ \rho + 10\alpha_N log(r) + \chi_N & \text{otherwise} \end{cases} \tag{4.6}$$

Table 4.1: Algorithm For Exhaustive Search

1. Set $N_{EX} = \frac{360^\circ}{BW^\circ_{EX}}$**.**
2. Set $i = 1$**.**
3. BS transmits pilot signal with beamwidth BW°_{EX} **in** i **for** T_{sig}**(s).**
4. UE estimates τ**.**
5. if $(\tau \geq \alpha_{th})$
6. Link established.
7. else {
8. if $(i \leq N_{EX})$
9. $i = i+1$**, wait for** T_{per}**(s) and repeat process from step 3.**
10. else
11. terminate. }

Here, ρ denotes a fixed path loss factor, α_L & α_N are the path loss exponents for LoS and NLoS mmWave links respectively, and χ_L & χ_N are the zero mean log normal random variables for LoS and NLoS mmWave links, respectively, which represent shadowing or blockage [57].

If UE receives a signal from the BS, then the power received, P_r, is expressed as

$$P_r = \frac{P_t G(\theta)\mu}{L_{mm}(r)}, \tag{4.7}$$

where P_t is the transmit power and μ is the squared envelope of multipath fading where the envelope follows a Rayleigh or Rician distribution depending on whether the UE-BS link is NLoS or LoS, respectively [57]. The SNR, τ is calculated as

$$\tau = \frac{P_r}{\sigma^2}, \tag{4.8}$$

where σ^2 represents the noise power. A decision regarding the establishment of a BS-UE link is made, such that

$$\begin{cases} \tau \geq \alpha_{th} & \text{Link established} \\ \tau < \alpha_{th} & \text{Link not established} \end{cases} \tag{4.9}$$

where α_{th} is the SNR threshold.

If UE is not present in a particular search sector, then the BS waits for T_{per} (s) and repeats the entire process for the next sector. This process continues until the BS has found UE, or the BS has searched in all sectors, i.e., $i = N_{EX}$, but could not find a UE. The algorithm is summarized in Table 4.1.

Assuming a UE has been detected with probability P_d, we now define the discovery delay, which is the time required to discover the user. For the sake of simplicity, we are considering only the effect of UE orientation and search beamwidth on discovery delay. Let UE be located at x° with respect to the BS, then the discovery delay for exhaustive search, DD_{EX}, is computed as

$$\begin{aligned} &DD_{EX} = (i)T_{sig} + (i-1)T_{per}, \text{ (for } i \in I) \\ &\text{subject to:} \\ &\tau \geq \alpha_{th} \end{aligned} \tag{4.10}$$

As an example, consider a UE located at 55° with respect to BS. Given that UE has been detected for $i = 6$ by using a $BW^\circ_{EX} = 10^\circ$ that covers the search space from $\theta^\circ_S = 50^\circ$ to $\theta^\circ_E = 60^\circ$; discovery delay for UE calculated using (4.10) is $DD_{EX} = 1060\mu$s (where $T_{sig} = 10\mu$s and $T_{per} = 200\mu$s [39]). This example is graphically shown in Fig. 4.1.

4.2 Iterative Search

Consider a BS searching for UE by deploying iterative search. Iterative search successively narrows down search beam until a suitable link with UE has been established. Let N_{IT} be a positive integer that denotes the number of search sectors, then

$$N_{IT} = m, \tag{4.11}$$

where m is a positive integer that can take on values that are greater than 1. For example, if the bisection method is used then $m = 2$ and the entire search area is divided into two beams, each having a beamwidth of 180°. On the other hand, if $m = 3$, then the entire search space will be covered using three beams, each having a beamwidth of 120°.

To understand iterative search, let us introduce the concept of $Stages$. Iterative search successively narrows down search beams; this narrowing down of search beam occurs in a particular stage, S. Let $Stages$ be the upper bound on the number of stages, i.e., $S \leq Stages$.[1]

If $BW^{\circ}_{IT_S}$ is the search beamwidth for a particular stage S, then

$$BW^{\circ}_{IT_S} = \frac{360^{\circ}}{m^S}, \tag{4.12}$$

[1]Note that $Stages$ is a design parameter. Its value depends on the narrowest allowable search beam that antenna arrays at the transmitter and receiver can support.

Table 4.2: Algorithm For Iterative Search

1. Set $S = 1$, where S represents the stage in hierarchical search.
2. Set $N_{IT} = m$.
3. Set $i = 1$.
4. Set $BW^{\circ}_{IT_S} = \frac{360^{\circ}}{m^S}$.
5. BS transmits pilot signal with beamwidth, $BW^{\circ}_{IT_S}$, in i for T_{sig}(s).
6. UE estimates τ.
7. if ($\tau \geq \alpha_{th}$)
8. Link established.
9. else if ($\tau \geq \alpha_S$) and ($S \leq Stages$)
10. $S = S + 1$ and repeat from step 3.
11. else {
12. if ($i \leq N_{IT}$)
13. $i = i + 1$, wait for T_{per}(s) and repeat from step 5.
14. else
15. terminate.}

A similar process to that of exhaustive search follows here. Let $I = \{1, ..., N_{IT}\}$, then the search space spanned by the beam for a particular $i \in I$ at a certain stage S is given by

$$\begin{aligned} \theta^{\circ}_S(S) &= (i-1)BW^{\circ}_{IT_S} + \theta^{\circ}_S(S-1), \\ \theta^{\circ}_E(S) &= (i)BW^{\circ}_{IT_S} + \theta^{\circ}_S(S-1), \end{aligned} \tag{4.13}$$

where $\theta^{\circ}_S(S)$ and $\theta^{\circ}_E(S)$ mark the beginning and end of the search beam at a certain level S for a particular $i \in I$ while $\theta^{\circ}_S(S-1)$ is the angular offset from the previous stage.

If UE has received signal from the BS, it measures τ by using Eqs. (4.3 –

4.8). Subsequently, we define the following scheme for link establishment

$$\begin{cases} \tau \geq \alpha_{th}, & \text{Link established} \\ \tau \geq \alpha_S, & \text{Narrow down search in this sector} \\ \tau < \alpha_S, & \text{UE is not present in this sector} \end{cases} \tag{4.14}$$

where α_{th} is the desired threshold at which a decision regarding the establishment of a link is made and α_S is a loose threshold that identifies the region that should be narrowed down to locate UE. The algorithm is summarized in Table 4.2.

The discovery delay for iterative algorithm is the sum of the delay incurred at a stage, DD_S, at which the UE has been tracked (i.e., $\tau \geq \alpha_S$) and the stage at which UE has been found (i.e., $\tau \geq \alpha_{th}$). Mathematically

$$\begin{aligned} & \quad DD_S = (i)T_{sig} + (i-1)T_{per}, \\ & \text{subject to:} \\ & \quad \tau \geq \alpha_{th} \\ & \text{and} \\ & \quad DD_S = (N_{IT})T_{sig} + (N_{IT}-1)T_{per}, \\ & \text{subject to:} \\ & \quad \tau \geq \alpha_S \end{aligned} \tag{4.15}$$

Hence, the total delay for iterative search, DD_{IT}, is defined as

$$DD_{IT} = \sum_{S=1}^{Stages} DD_S, \tag{4.16}$$

subject to the constraint that UE has been detected.

Example

Assume the use of bisection method, i.e., $m = 2$; bisection method bisects the search space and selects the region where UE lies for further processing. The process continues until UE has been found or $S > Stages$. Consider a UE located at $55°$ with respect to the BS. Let $Stages = 4$, and initial condition $\theta^{\circ}_S(0) = 0°$, then search starts with

$$\begin{cases} S = 1, \\ BW^{\circ}_{IT_1} = 180°, \text{ (using (4.12))} \\ i = 1, \\ \theta^{\circ}_S(1) = 0°, \text{ (using (4.13))} \\ \theta^{\circ}_E(1) = 180°, \\ i = 2, \\ \theta^{\circ}_S(1) = 180°, \\ \theta^{\circ}_E(1) = 360°, \end{cases}$$

Let $\tau \geq \alpha_S$ for $i = 1$, then discovery delay calculated using (4.15) is $DD_1 = 220\mu$s. Since $S \leq Stages$ and $\tau < \alpha_{th}$, we proceed to the next step.

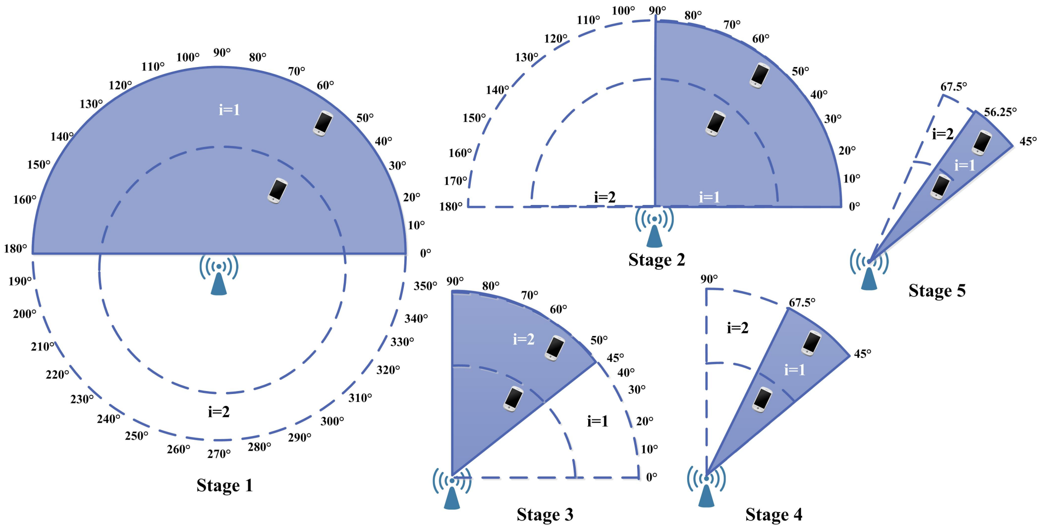

Figure 4.2: Iterative Search.

$$\begin{cases} S = 2, \\ BW^{\circ}_{IT_2} = 90^{\circ}, \\ i = 1, \\ \theta^{\circ}_{S}(2) = 0^{\circ} + \theta^{\circ}_{S}(1), \text{ (since } \theta^{\circ}_{S}(1) = 0^{\circ}) \\ \theta^{\circ}_{E}(2) = 90^{\circ} + \theta^{\circ}_{S}(1), \\ i = 2, \\ \theta^{\circ}_{S}(2) = 90^{\circ} + \theta^{\circ}_{S}(1), \\ \theta^{\circ}_{E}(2) = 180^{\circ} + \theta^{\circ}_{S}(1), \end{cases}$$

Similarly, if $\tau \geq \alpha_S$ for $i = 1$, then DD_2, using (4.15), is 220μs and next stage begins.

$$\begin{cases} S = 3, \\ BW^{\circ}_{IT_3} = 45^{\circ}, \\ i = 1, \\ \theta^{\circ}_{S}(3) = 0^{\circ} + \theta^{\circ}_{S}(2), \text{ (since } \theta^{\circ}_{S}(2) = 0^{\circ}) \\ \theta^{\circ}_{E}(3) = 45^{\circ} + \theta^{\circ}_{S}(2), \\ i = 2, \\ \theta^{\circ}_{S}(3) = 45^{\circ} + \theta^{\circ}_{S}(2), \\ \theta^{\circ}_{E}(3) = 90^{\circ} + \theta^{\circ}_{S}(2), \end{cases}$$

Likewise, $\tau \geq \alpha_S$ for $i = 2$, discovery delay for $S = 3$ is $DD_3 = 220\mu$s.

$$\begin{cases} S = 4, \\ BW^{\circ}_{IT_4} = 22.5^{\circ}, \\ i = 1, \\ \theta^{\circ}_{S}(4) = 45^{\circ} + \theta^{\circ}_{S}(3), \text{ (since } \theta^{\circ}_{S}(3) = 0^{\circ}) \\ \theta^{\circ}_{E}(4) = 67.5^{\circ} + \theta^{\circ}_{S}(3), \\ i = 2, \\ \theta^{\circ}_{S}(4) = 67.5^{\circ} + \theta^{\circ}_{S}(3), \\ \theta^{\circ}_{E}(4) = 90^{\circ} + \theta^{\circ}_{S}(3), \end{cases}$$

If $\tau \geq \alpha_{th}$, then a link between BS-UE has been established. The total discovery delay in the view of above example is

$$DD_{IT} = DD_1 + DD_2 + DD_3 + DD_4 = 670\mu s,$$

Otherwise, if $\tau < \alpha_{th}$ at $S = 4$, the search process terminates and this becomes a case of misdetection. This example case is summarized in Fig.

4.2.

4.3 Hybrid Search

We aim to combine the strengths of exhaustive search and iterative search and propose a *hybrid* algorithm that outperforms iterative in terms of misdetection probability and exhaustive in terms of discovery delay.

To be precise, the BS first implements iterative search after which exhaustive search begins. Let N_{HY} be a positive integer that defines the number of search sectors, such that

$$N_{HY} = \begin{cases} \quad N_{IT} = m, \\ \text{subject to:} \\ \quad S \leq Stages, \ \tau < \alpha_{th} \\ \\ \quad N_{EX} = \frac{BW^{\circ}_{IT_S}}{BW^{\circ}_{EX}}, \\ \text{subject to:} \\ \quad S > Stages, \ \tau < \alpha_{th} \end{cases} \tag{4.17}$$

Iterative search tracks down UE by using wide beams. Following that, exhaustive search exhaustively scans the targeted region in order to establish a suitable link. Let us define BW°_{HY} as the search beam for hybrid scheme, then

$$BW^{\circ}_{HY} = \begin{cases} \quad BW^{\circ}_{IT_S} = \frac{360^{\circ}}{m^S} \\ \text{subject to:} \\ \quad S \leq Stages,\ \tau < \alpha_{th} \\ \\ \quad BW^{\circ}_{EX} \\ \text{subject to:} \\ \quad S > Stages,\ \tau < \alpha_{th} \end{cases} \tag{4.18}$$

Following in the footsteps of exhaustive and iterative search, let us define $I = \{1, ..., N_{HY}\}$. The region spanned by the beam for a particular $i \in I$ at a specific stage, S, is given as

$$\begin{aligned} \theta^{\circ}_{S}(S) &= (i-1)BW^{\circ}_{HY} + \theta^{\circ}_{S}(S-1), \\ \theta^{\circ}_{E}(S) &= (i)BW^{\circ}_{HY} + \theta^{\circ}_{S}(S-1), \end{aligned} \tag{4.19}$$

If UE is present in the current sector of search, then τ is measured using Eqs. (4.3 – 4.8). The decision regarding the establishment of a UE-BS link is made using (4.14). The algorithm is summarized in Table 4.3. Discovery delay for hybrid search, DD_{HY}, is

$$DD_{HY} = DD_{IT} + DD_{EX}, \tag{4.20}$$

where DD_{EX} is calculated using (4.10) and DD_{IT} is given by (4.15, 4.16).

Table 4.3: Algorithm For Hybrid Search

1. Set $S = 1$, where S represents the stage in hierarchical search.
2. Set $N_{HY} = m$ sectors.
3. Set $BW^{\circ}_{IT_S} = \frac{360^{\circ}}{m^S}$ and $BW^{\circ}_{HY} = BW^{\circ}_{IT_S}$.
4. Set $i = 1$.
5. BS transmits pilot signal with beamwidth, BW°_{HY}, in i for T_{sig}(s).
6. UE estimates τ.
7. if $(\tau \geq \alpha_{th})$
8. Link established.
9. else if $(\tau \geq \alpha_S)$ and $(S \leq Stages)$
10. $S = S + 1$, repeat from step 3.
11. else if $(S > Stages)$
12. Start exhaustive search.
13. Set $BW^{\circ}_{HY} = BW^{\circ}_{EX}$.
14. Set $N_{HY} = \frac{BW^{\circ}_{IT_S}}{BW^{\circ}_{EX}}$ and repeat from step 4.
15. else {
16. if $(i \leq N_{HY})$
17. $i = i + 1$, wait for T_{per}(s), and repeat from step 5.
18. else
19. terminate.}

Example

Consider an example wherein UE is situated 55° with respect to the BS. Let $m = 2$, $Stages = 3$, $BW^{\circ}_{EX} = 10^{\circ}$, and initial condition $\theta^{\circ}_{S}(0) = 0^{\circ}$. The search begins with

$$\begin{cases} N_{HY} = N_{IT} = 2, \\ S = 1, \\ BW^{\circ}_{HY} = BW^{\circ}_{IT_1} = 180^{\circ}, \\ i = 1, \\ \theta^{\circ}_{S}(1) = 0^{\circ}, \\ \theta^{\circ}_{E}(1) = 180^{\circ}, \\ i = 2, \\ \theta^{\circ}_{S}(1) = 180^{\circ}, \\ \theta^{\circ}_{E}(1) = 360^{\circ}, \end{cases}$$

Let $\tau \geq \alpha_S$ for $i = 1$. The delay incurred at $S = 1$, using (4.15), is 220μs. Since a suitable link has not been established, so the next stages begins.

$$\begin{cases} N_{HY} = N_{IT} = 2, \\ S = 2, \\ BW^{\circ}_{HY} = BW^{\circ}_{IT_2} = 90^{\circ}, \\ i = 1, \\ \theta^{\circ}_{S}(2) = 0^{\circ} + \theta^{\circ}_{S}(1),\ (\text{since } \theta^{\circ}_{S}(1) = 0^{\circ}) \\ \theta^{\circ}_{E}(2) = 90^{\circ} + \theta^{\circ}_{S}(1), \\ i = 2, \\ \theta^{\circ}_{S}(2) = 90^{\circ} + \theta^{\circ}_{S}(1), \\ \theta^{\circ}_{E}(2) = 180^{\circ} + \theta^{\circ}_{S}(1), \end{cases}$$

Assume $\tau \geq \alpha_S$ for $i = 1$, the delay incurred at $S = 2$ is 220μs (using Eq.

4.15). Since $S \leq Stages$, the next stage begins.

$$\begin{cases} N_{HY} = N_{IT} = 2, \\ S = 3, \\ BW^{\circ}_{HY} = BW^{\circ}_{IT_3} = 45^{\circ}, \\ i = 1, \\ \theta^{\circ}_{S}(3) = 0^{\circ} + \theta^{\circ}_{S}(2),\ (\text{since}\ \theta^{\circ}_{S}(2) = 0^{\circ}) \\ \theta^{\circ}_{E}(3) = 45^{\circ} + \theta^{\circ}_{S}(2), \\ i = 2, \\ \theta^{\circ}_{S}(3) = 45^{\circ} + \theta^{\circ}_{S}(2), \\ \theta^{\circ}_{E}(3) = 90^{\circ} + \theta^{\circ}_{S}(2), \end{cases}$$

Suppose $\tau \geq \alpha_S$ for $i = 2$, but link has not been established. Since $S = Stages$, exhaustive search starts. Note that delay incurred at $S = 3$ is 220μs.

$$\begin{cases} N_{HY} = N_{EX} \approx 5, \\ BW^{\circ}_{HY} = BW^{\circ}_{EX} = 10^{\circ}, \\ i = 1, \\ \theta^{\circ}_{S}(4) = 45^{\circ} + \theta^{\circ}_{S}(3), \ \text{(since } \theta^{\circ}_{S}(3) = 0^{\circ}\text{)} \\ \theta^{\circ}_{E}(4) = 55^{\circ} + \theta^{\circ}_{S}(3), \\ i = 2, \\ \theta^{\circ}_{S}(4) = 55^{\circ} + \theta^{\circ}_{S}(3), \\ \theta^{\circ}_{E}(4) = 65^{\circ} + \theta^{\circ}_{S}(3), \\ i = 3, \\ \theta^{\circ}_{S}(4) = 65^{\circ} + \theta^{\circ}_{S}(3), \\ \theta^{\circ}_{E}(4) = 75^{\circ} + \theta^{\circ}_{S}(3), \\ i = 4, \\ \theta^{\circ}_{S}(4) = 75^{\circ} + \theta^{\circ}_{S}(3), \\ \theta^{\circ}_{E}(4) = 85^{\circ} + \theta^{\circ}_{S}(3), \\ i = 5, \\ \theta^{\circ}_{S}(4) = 85^{\circ} + \theta^{\circ}_{S}(3), \\ \theta^{\circ}_{E}(4) = 90^{\circ} + \theta^{\circ}_{S}(3), \end{cases}$$

Assuming $\tau \geq \alpha_{th}$ for $i = 2$, a suitable link between BS and UE has been established. The delay experienced at this level is 220μs (using Eq. 4.10). The total delay is the sum of the delays experienced during both iterative and exhaustive search, and is found to be 880μs (using (4.20)). This example is pictorially shown in Fig. 4.3.

Having discussed the three cell search algorithms, we next move towards performing a comparative analysis among them in order to show the balanced

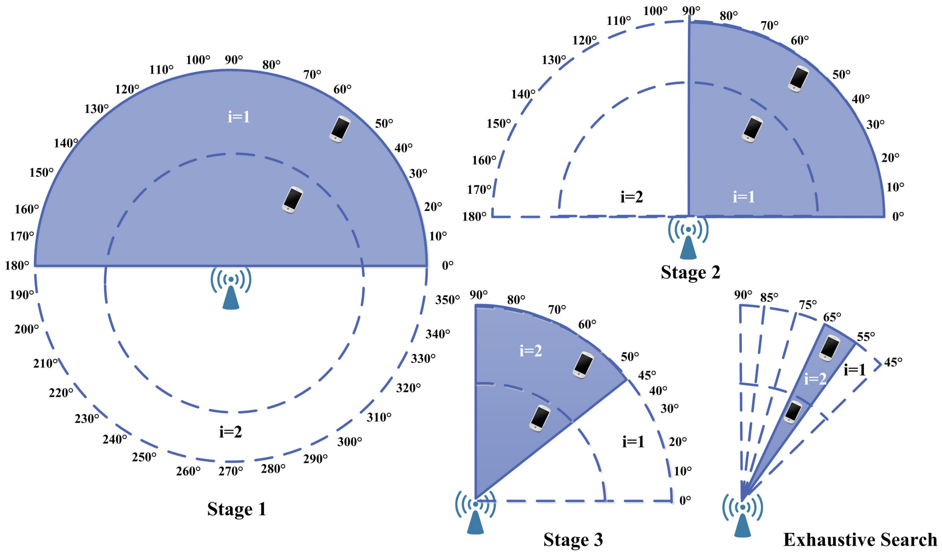

Figure 4.3: Hybrid Search.

trade-off between detection probability and discovery delay that is achieved by hybrid algorithm.

Chapter 5

Comparative Analysis

> **"If you have built castles in the air, your work need not be lost; that is where they should be. Now put the foundations under them."— Henry David Thoreau**

5.1 Simulation Environment

In harmony with Henry's thoughts, we next explain the simulation environment developed for the purpose of performance evaluation. We have ignored rain attenuation, atmospheric, and molecular absorption losses since these losses do not add any significant additional path loss within a cell radius of 200m, which is the cell size in our scenario. Next, we assume that BSs can produce a beam of $5°$, $10°$, and $20°$ [79]. It is important to mention that mmWave systems provide sparse scattering environment and are used in combination with μ-Wave BS in order to reduce the problem of intermittency in the mmWave links. Our system model contains only one mmWave

Table 5.1: Simulation Parameters

f_c	73 GHz
P_t	30dBm
E	Assuming 100%
Gtx	24.5 dBi
Grx	24.5 dBi
UE position	Randomly generated (unless stated otherwise)
BF	Analog beamforming.
T_{sig}	10 μs
T_{per}	200 μs
α_S	20 dB
α_{th}	40 dB (unless stated otherwise)
NF	10dB

BS and one UE, and the problem of intermittency in the links has been incorporated by appropriate channel modeling. This assumption of one BS and one UE is in accordance with [12]. The design of synchronization signal used in the simulation environment is same as shown in Fig. 3.2. For simplicity, we consider that BS implements analog beamforming.

The performance of the three algorithms is compared in terms of two parameters: misdetection probability and discovery delay, which are measured against varying SNR, distance, and UE orientation. Misdetection probability depends on a number of factors, such as distance, received SNR, search beam width, and LoS or NLoS channel. In our simulations, channel is generated as LoS or NLoS by following a uniform random distribution and approximated using Monte Carlo simulations (10^5 times). The simulation parameters are summarized in Table 5.1. Once a UE has been detected then discovery delay depends on user orientation with respect to the BS and the search beam width used.

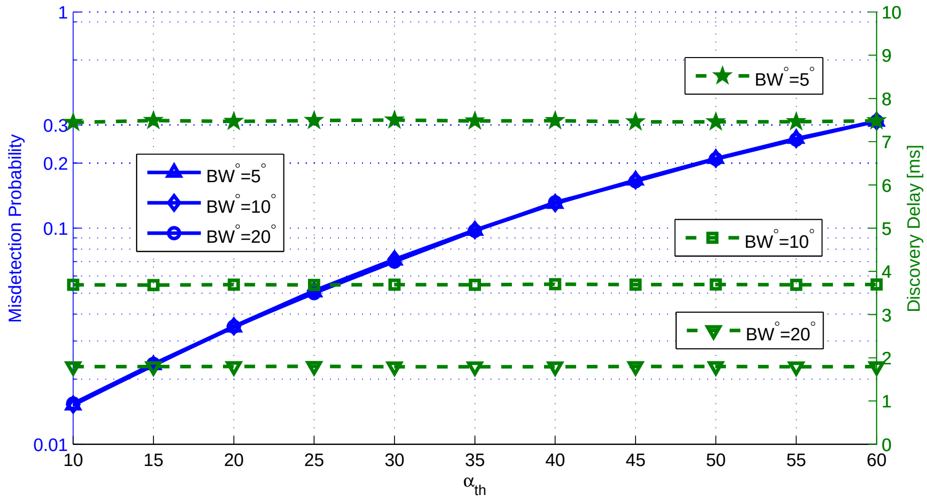

Figure 5.1: Exhaustive Search vs α_{th} for BW° = 5°, 10°, and 20°.

5.2 Effect of SNR

We first discuss the effect of using different search beams on misdetection probability and discovery delay. For this purpose, we vary α_{th}, and plot misdetection probability and discovery delay for exhaustive, iterative, and hybrid search schemes in Fig. 5.1, 5.2, and Fig. 5.3 respectively. Note that UE can be located anywhere in the cell at a fixed distance of $r = 95m$ (in order to see the performance at edge users).

Consider a BS that is implementing exhaustive search. It is searching for a UE by using three different beamwidths: 5°, 10°, and 20°. The corresponding misdetection probability and discovery delay are plotted in Fig. 5.1. It can be seen that among the three search beams, using a 20° is most efficient because it provides low discovery delay while having same misdetection probability as a 5° beam. In terms of hardware constraints, creating a 5° beam consumes more power and energy in comparison to a 20° beam. Thus, the selection of

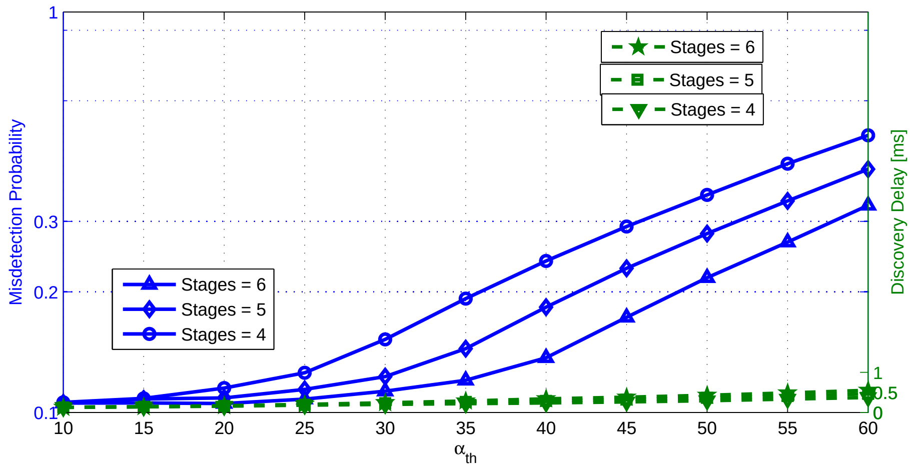

Figure 5.2: Iterative Search vs α_{th} for Stages = 6, 5 and 4.

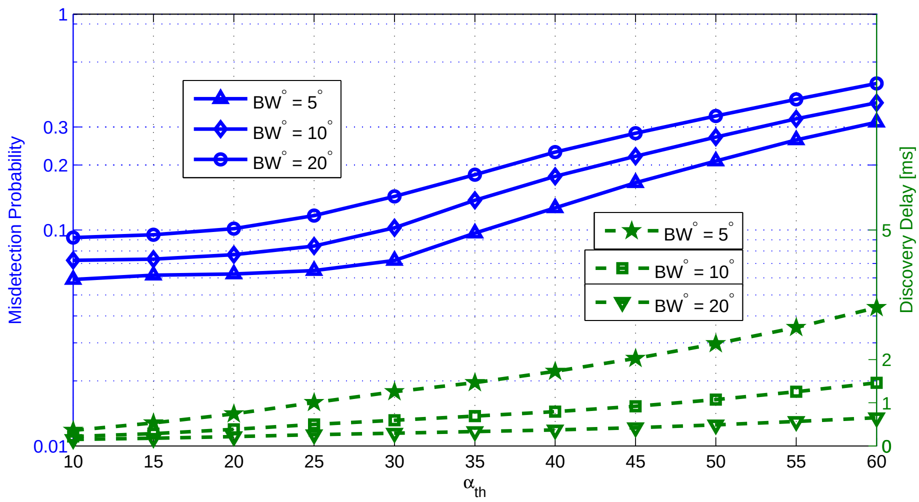

Figure 5.3: Hybrid Search vs α_{th} for BW° = 5°, 10°, and 20°.

an appropriate search beam depends on a particular environment and using a narrowest beam for search may not be optimal in some cases.

In order to produce the desired search beams of 5°, 10°, and 20° using a BS that is deploying iterative search; the number of *Stages* need to be controlled. In particular, $Stages = 6, 5$, and 4 will create the required beams as shown in Fig. 5.2. It can be seen from the figure that discovery delay using iterative search is same for all three beamwidths, but there is a difference in misdetection probability. Since the main aim is to discover UE and discovery delay for all three search beams is same, thus $Stages = 6$ or $BW^{\circ}_{IT_6} = 5.625^{\circ}$ is the best choice in this case. The same explanation follows for hybrid search, where $Stages = 3$ is fixed and different search beams are used.

Comparison

Without loss of generality, we have fixed the narrowest allowable search beam at 10° in order to have a fair comparison [9]. Thus, $BW^{\circ}_{EX} = 10^{\circ}$ for exhaustive search, which is equivalent to $m = 2$, $Stages = 5$ for iterative search. Similarly, $BW^{\circ}_{EX} = 10^{\circ}$, $m = 2$, and $Stages = 3$ for hybrid search. The results are plotted in Fig. 5.4. It can be seen that hybrid lies midway between exhaustive and iterative in terms of its performance. Moreover, Fig. 5.5 shows two sets of results; one set is plotted at $r = 10$m and the second at $r = 95$m. It can be seen that misdetection probability is low at 10m as compared to 95m, which is intuitive because of a decrease in SNR for the latter case. Note that each simulation point on the graph is estimated using Monte Carlo simulation with 10^5 iterations. Again note that exhaustive

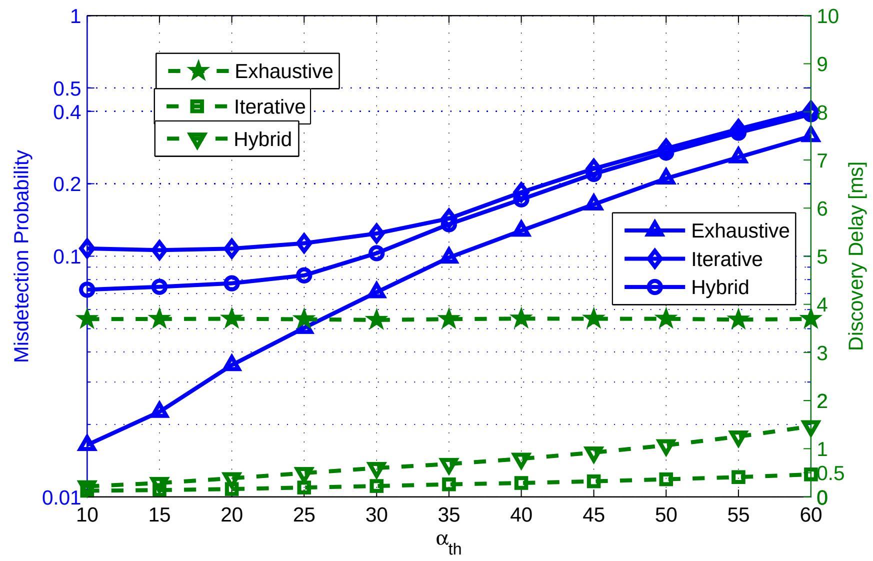

Figure 5.4: Comparison between exhaustive, iterative, and hybrid with regard to α_{th} for BW° = 10°.

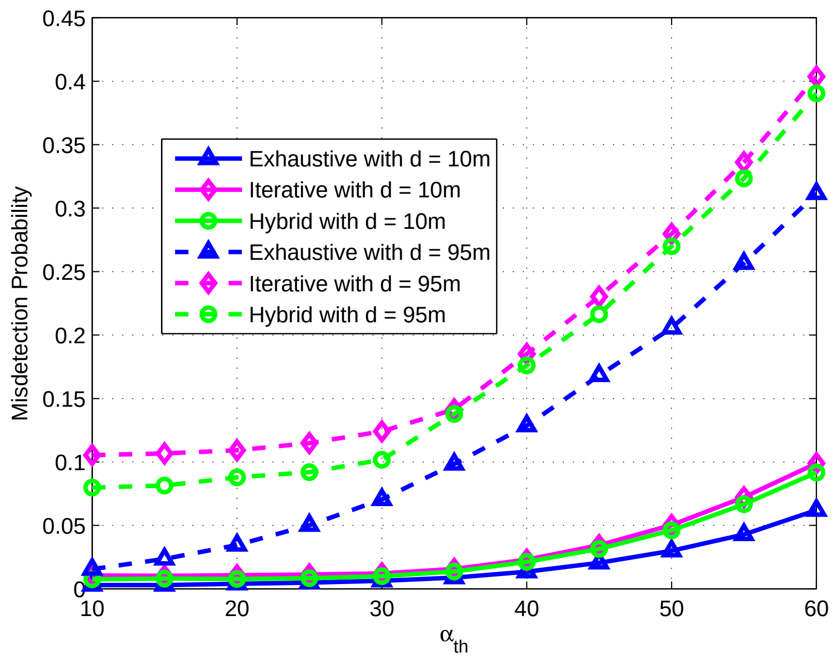

Figure 5.5: Comparison between exhaustive, iterative, and hybrid with regard to α_{th} for BW° = 10° at d = 10m and d = 95m.

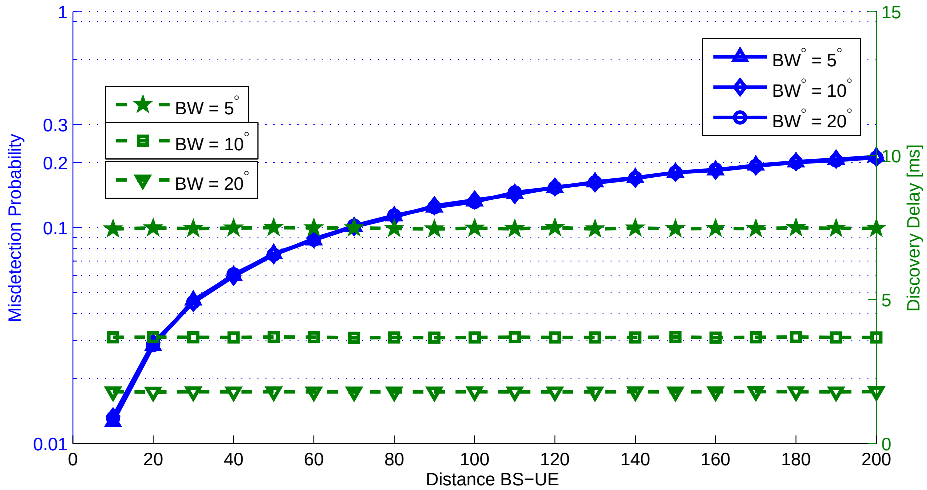

Figure 5.6: Exhaustive search vs distance for BW° = 5°, 10°, and 20°.

search provides the lowest misdetection probability while the proposed hybrid algorithm lies in between exhaustive and iterative in terms of performance.

5.3 Effect of Distance

Next, we study the effect of distance on misdetection probability. For this purpose, we increase the distance between BS and UE in 10m increments from 10m to 200m. In this case, we have fixed α_{th} at 40dB. In order to see the effect of using $BW^\circ = 5^\circ, 10^\circ$, and 20° for a particular cell search algorithm with varying distance, we have plotted the results in Fig. 5.6, Fig. 5.7, and Fig. 5.8.

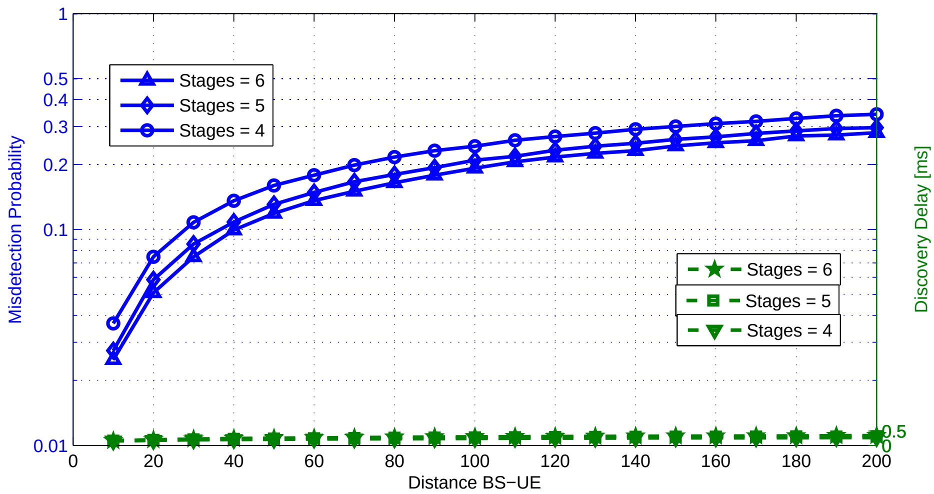

Figure 5.7: Iterative search vs distance for Stages = 6, 5, and 4.

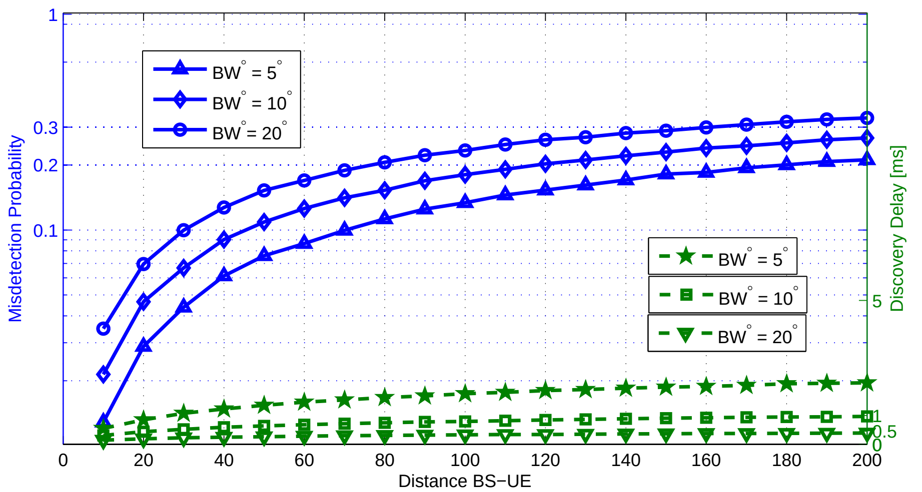

Figure 5.8: Hybrid search vs distance for BW° = 5°, 10°, and 20°.

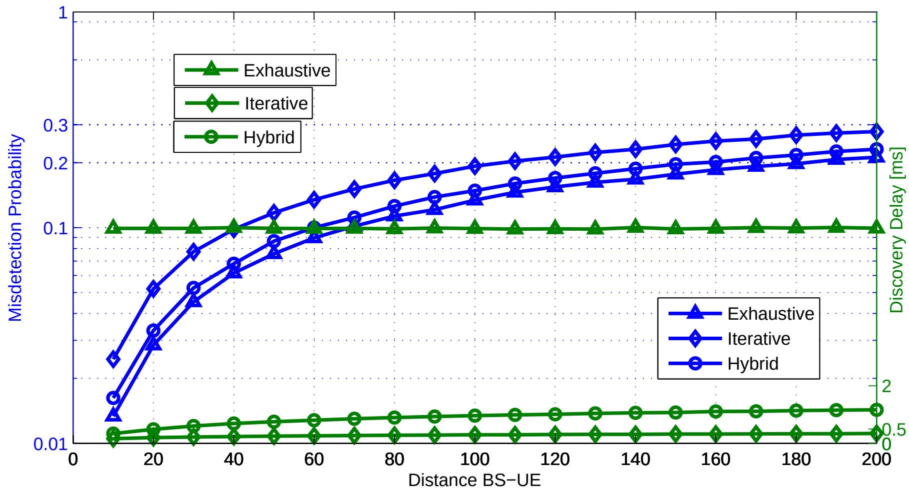

Figure 5.9: Comparison between exhaustive, iterative, and hybrid with regard to distance for BW° = 10°.

Comparison

A comparison among the three cell search schemes for increasing distance is shown in Fig. 5.9. It can be seen from the figure that misdetection probability increases with increasing distance and hybrid algorithm lies mid-way between exhaustive and iterative in terms of its performance. Once the UE has been detected, the discovery delay is calculated using respective equations for exhaustive, iterative, and hybrid algorithms and averaged over 10^5 trials. It can be seen that exhaustive search has high discovery delay (around 7.5ms) in comparison to iterative and hybrid schemes.

5.4 Effect of UE Orientation

Following this, we study the effect of UE orientation on misdetection probability and discovery delay. To do that, we vary the position of UE from 9°

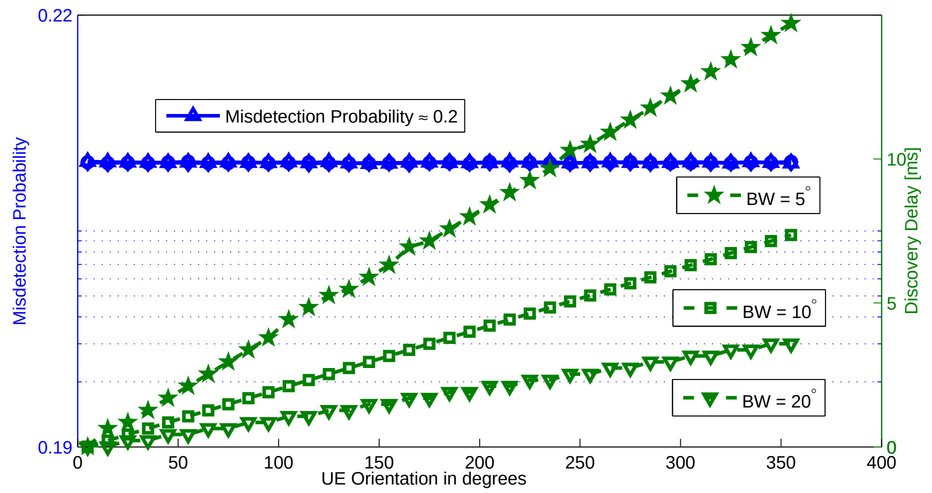

Figure 5.10: Exhaustive vs UE orientation for BW° = 5°, 10°, and 20°.

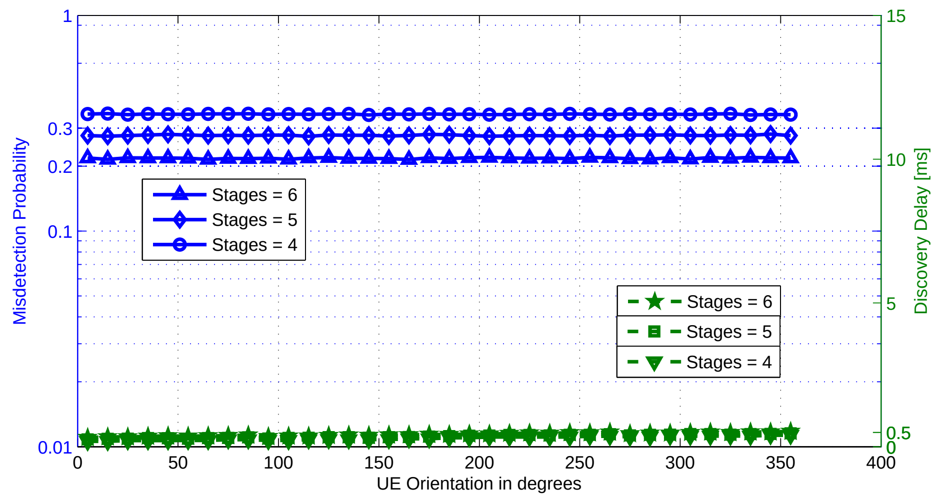

Figure 5.11: Iterative vs UE orientation for Stages = 6, 5, and 4.

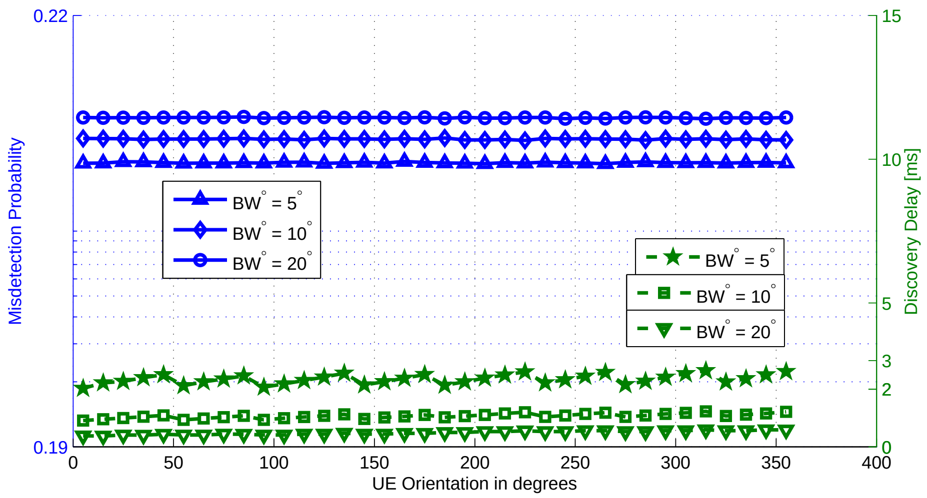

Figure 5.12: Hybrid vs UE orientation for BW° = 5°, 10°, and 20°.

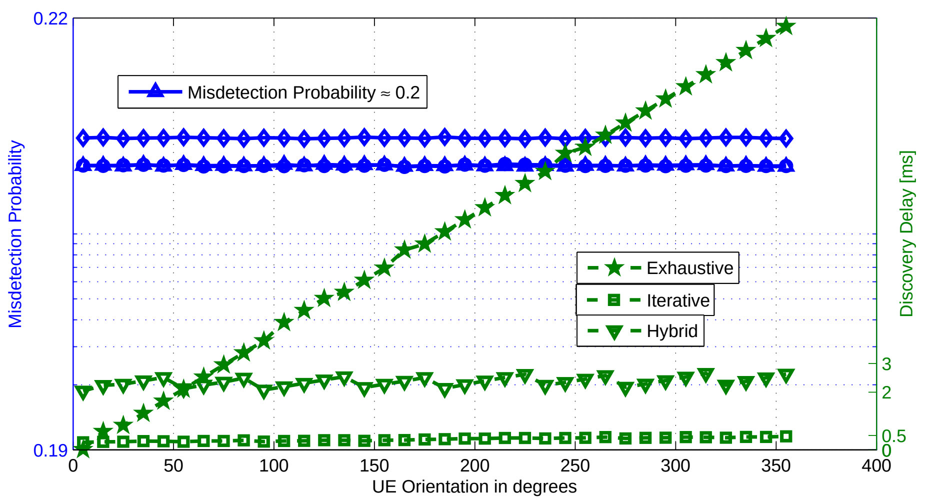

Figure 5.13: Comparison between exhaustive, iterative, and hybrid with regard to UE orientation for BW° = 10°.

Table 5.2: Comparison between Cell Search Algorithms

Issue of Interest	***Exhaustive***	***Iterative***	***Hybrid***
Detection Probability	High	Reasonable	Reasonable
Discovery Delay	High	Low	Reasonable
Robustness to UE orientation	No	Yes	Yes
Degrees of freedom	One	Two	Three

to 359° in 10° increments. We have fixed the radius at $r = 95$m to see the algorithm's performance for edge users. The discussion in this section follow suit. The effect of using different search beams with a particular cell search algorithm is shown in Fig. 5.10, Fig. 5.11, and Fig. 5.12.

Comparison

In order to do a comparative analysis between the three algorithms, we are using $\alpha_{th} = 50$dB since this is a threshold at which all three algorithms give same misdetection probability. With all three algorithms having same misdetection probability, we can easily see an algorithm's robustness to initial UE orientation. This is due to the fact that once the orientation of user is determined, the BS saves it location and no search is required next time given that UE is not mobile and has not changed its location. The results are plotted in Fig. 5.13. It can be seen that exhaustive search is most sensitive to initial UE orientation while iterative and hybrid are relatively robust to this parameter. The misdetection probability for all three algorithms lie within acceptable limits (i.e., 0.2).

Another very interesting insight that can be inferred from the above discussion is that hybrid algorithm offer more degrees of freedom in comparison to exhaustive and iterative. Depending on the dynamics of the location, hybrid algorithm can be adjusted to meet the performance specifications. The main conclusions deduced from the simulation results are summarized in Table 5.2.

Chapter 6

Conclusions and Future Work

> **"If you're walking down the right path and you're willing to keep walking, eventually you'll make progress."— Barack Obama**

In this dissertation, we first discussed the key characteristics of mmWave systems that distinguish them from legacy systems. These noticeable features are high isotropic path loss, which is compensated for by using directional transmission. Due to small wavelengths and directionality, mmWave systems are highly sensitive to blockage by humans as well as obstacle. Thus, coordination mechanisms become a key concern with mmWaves. In particular, this work focused on IA. The existing literature on IA scheme of LTE helped in providing the design of synchronization signal, which was later used in designing the novel cell search algorithm. The developed algorithm, called hybrid algorithm, combined the strengths of exhaustive and iterative schemes, thereby achieving a high detection probability than iterative search and low discovery delay than exhaustive search. This result was validated by measuring the detection probability and discovery delay against three parameters that are α_{th}, distance, and UE orientation. The simulation results show that hybrid search achieves a performance that is better than exhaustive in terms of discovery delay and has good detection probability in comparison to iterative.

The suitability of a particular beamforming design, i.e., analog , digital, and hybrid architecture for a specific environment is a critical design concern. As part of our future work, we aim to investigate the performance of cell search algorithms with digital and hybrid architectures. The major effect of using a digital or hybrid architecture is in terms of discovery delay as digital and hybrid allows the use of multiple beams per time slot. Furthermore, the use of reconfigurable antennas will provide much more flexibility than fixed antenna gains [22], this is another area ripe for research. As mmWave systems are highly sensitive to blockage, so the idea of using backup BS that could be used in the case when connection with primary BS is lost or for the purpose of smooth handover is another exciting venture in this domain [40]. We aim to investigate these issues as part of our future work.

Bibliography

[1] E-band technology. E-band Communications. *Available: http://www.e-band.com/index.php?id=86*.

[2] http://wireless.engineering.nyu.edu/.

[3] http://www.profheath.org/.

[4] IEEE 802.15 WPAN Task Group 3c (tg3c) Millimeter Wave Alternative PHY. *Available: http://www.ieee802.org/15/pub/TG3c.html*.

[5] Understanding millimeter wave wireless communication. *Available: http://www.loeacom.com/pdf*.

[6] Draft Standard for Information Technology-Telecommunications and Information Exchange Between Systems-Local and Metropolitan Area Networks-Specific Requirements-Part11: Wireless LAN Medium Access Control (MAC) and Physical Layer (PHY) Specifications-Amendment 4: Enhancements for Very High Throughput in the 60 GHz Band, IEEEP802.11ad/D9.0. Oct, 2012.

[7] Zohair Abu-Shaban, Henk Wymeersch, Xiangyun Zhou, Gonzalo Seco-Granados, and Thushara Abhayapala. Random-Phase Beamforming for Initial Access in the Millimeter-Wave Cellular Networks.

[8] Hossein Ajorloo and Mohammad Taghi Manzuri-Shalmani. Modeling beacon period length of the UWB and 60-GHz mmwave WPANs based on ECMA-368 and ECMA-387 standards. *IEEE Transactions on Mobile Computing*, 12(6):1201–1213, 2013.

[9] Mustafa Riza Akdeniz, Yuanpeng Liu, Mathew K Samimi, Shu Sun, Sundeep Rangan, Theodore S Rappaport, and Elza Erkip. Millimeter wave channel modeling and cellular capacity evaluation. *IEEE Journal on Selected Areas in Communications*, 32(6):1164–1179, 2014.

[10] Sayf Alalusi and Robert Brodersen. A 60ghz phased array in CMOS. In *Custom Integrated Circuits Conference, 2006. CICC'06. IEEE*, pages 393–396. IEEE, 2006.

[11] Ana Vázquez Alejos, Manuel GarcÍa Sanchez, and IÑigo Cuinas. Measurement and analysis of propagation mechanisms at 40 GHz: Viability of site shielding forced by obstacles. *IEEE Transactions on Vehicular Technology*, 57(6):3369–3380, 2008.

[12] Ahmed Alkhateeb, Omar El Ayach, Geert Leus, and Robert W Heath. Channel estimation and hybrid precoding for millimeter wave cellular systems. *IEEE Journal of Selected Topics in Signal Processing*, 8(5):831–846, 2014.

[13] KC Allen, N DeMinco, JR Hoffman, Y Lo, and P Papazian. Building penetration loss measurements at 900 MHz, 11.4 GHz, and 28.8 GHz. *US Department of Commerce, National Telecommunications and Information Administration Rep*, pages 94–306, 1994.

[14] Christopher R Anderson and Theodore S Rappaport. In-building wideband partition loss measurements at 2.5 and 60 GHz. *IEEE Transactions on Wireless Communications*, 3(3):922–928, 2004.

[15] Jeffrey G Andrews, Stefano Buzzi, Wan Choi, Stephen V Hanly, Angel Lozano, Anthony CK Soong, and Jianzhong Charlie Zhang. What will 5G be? *IEEE Journal on selected areas in communications*, 32(6):1065–1082, 2014.

[16] Yaniv Azar, George N Wong, Kevin Wang, Rimma Mayzus, Jocelyn K Schulz, Hang Zhao, Felix Gutierrez, DuckDong Hwang, and Theodore S Rappaport. 28 GHz propagation measurements for outdoor cellular communications using steerable beam antennas in New York City. In *Communications (ICC), 2013 IEEE International Conference on*, pages 5143–5147. IEEE, 2013.

[17] S. Sesia C. van Rensburg B. Clerckx, A. Lozano and C. B. Papadias. 3GPP LTE and LTE-advanced. *EURASIP Journal on Wireless Communications and Networking, vol. 2009*, 2009.

[18] Tianyang Bai, Rahul Vaze, and Robert W Heath. Analysis of blockage effects on urban cellular networks. *IEEE Transactions on Wireless Communications*, 13(9):5070–5083, 2014.

[19] C Nicolas Barati, S Amir Hosseini, Sundeep Rangan, Pei Liu, Thanasis Korakis, and Shivendra S Panwar. Directional cell search for millimeter wave cellular systems. In *Signal Processing Advances in Wireless Communications (SPAWC), 2014 IEEE 15th International Workshop on*, pages 120–124. IEEE, 2014.

[20] C Nicolas Barati, S Amir Hosseini, Sundeep Rangan, Pei Liu, Thanasis Korakis, Shivendra S Panwar, and Theodore S Rappaport. Directional cell discovery in millimeter wave cellular networks. *IEEE Transactions on Wireless Communications*, 14(12):6664–6678, 2015.

[21] Eshar Ben-Dor, Theodore S Rappaport, Yijun Qiao, and Samuel J Lauffenburger. Millimeter-wave 60 GHz outdoor and vehicle AOA propagation measurements using a broadband channel sounder. In *Global Telecommunications Conference (GLOBECOM 2011), 2011 IEEE*, pages 1–6. IEEE, 2011.

[22] Jennifer T Bernhard. Reconfigurable antennas. *Synthesis lectures on antennas*, 2(1):1–66, 2007.

[23] Federico Boccardi, Robert W Heath, Angel Lozano, Thomas L Marzetta, and Petar Popovski. Five disruptive technology directions for 5G. *IEEE Communications Magazine*, 52(2):74–80, 2014.

[24] Antonio Capone, Ilario Filippini, and Vincenzo Sciancalepore. Context information for fast cell discovery in mm-wave 5G networks. In *European Wireless 2015; 21th European Wireless Conference; Proceedings of*, pages 1–6. VDE, 2015.

[25] Margaret Chiosi, Don Clarke, Peter Willis, Andy Reid, James Feger, Michael Bugenhagen, Waqar Khan, Michael Fargano, Chunfeng Cui, Hui Deng, et al. Network functions virtualisation: An introduction, benefits, enablers, challenges and call for action. In *SDN and OpenFlow World Congress*, pages 22–24, 2012.

[26] Romit Roy Choudhury and Nitin H Vaidya. Deafness: A MAC problem in ad hoc networks when using directional antennas. In *Network protocols, 2004. ICNP 2004. Proceedings of the 12th IEEE international conference on*, pages 283–292. IEEE, 2004.

[27] I Cisco. Cisco visual networking index: Forecast and methodology, 2011–2016. *CISCO White paper*, pages 2011–2016, 2012.

[28] M Scott Corson, Rajiv Laroia, Junyi Li, Vincent Park, Tom Richardson, and George Tsirtsis. Toward proximity-aware internetworking. *IEEE Wireless Communications*, 17(6), 2010.

[29] Erik Dahlman, Stefan Parkvall, Johan Skold, and Per Beming. *3G evolution: HSPA and LTE for mobile broadband.* Academic press, 2010.

[30] Robert C Daniels, James N Murdock, Theodore S Rappaport, and Robert W Heath. 60 GHz wireless: Up close and personal. *IEEE Microwave Magazine*, 11(7):44–50, 2010.

[31] Cedric Dehos, Jose Luis González, Antonio De Domenico, Dimitri Kténas, and Laurent Dussopt. Millimeter-wave access and backhauling: the solution to the exponential data traffic increase in 5G mobile

communications systems? *IEEE Communications Magazine*, 52(9):88–95, 2014.

[32] Chinh H Doan, Sohrab Emami, David A Sobel, Ali M Niknejad, and Robert W Brodersen. Design considerations for 60 GHz CMOS radios. *IEEE Communications Magazine*, 42(12):132–140, 2004.

[33] Maged Elkashlan, Trung Q Duong, and Hsiao-Hwa Chen. Millimeter-wave communications for 5G: fundamentals: Part I [Guest Editorial]. *IEEE Communications Magazine*, 52(9):52–54, 2014.

[34] Maged Elkashlan, Trung Q Duong, and Hsiao-Hwa Chen. Millimeter-wave communications for 5G–part 2: applications [Guest Editorial]. *IEEE Communications Magazine*, 53(1):166–167, 2015.

[35] ISGNFV ETSI. Network Functions Virtualisation–Network Operator Perspectives on Industry Progress. *Updated White Paper*, 2013.

[36] Open Networking Fundation. Software-defined networking: The new norm for networks. *ONF White Paper*, 2:2–6, 2012.

[37] Suiyan Geng, Jarmo Kivinen, Xiongwen Zhao, and Pertti Vainikainen. Millimeter-wave propagation channel characterization for short-range wireless communications. *IEEE Transactions on Vehicular Technology*, 58(1):3–13, 2009.

[38] Amitava Ghosh, Timothy A Thomas, Mark C Cudak, Rapeepat Ratasuk, Prakash Moorut, Frederick W Vook, Theodore S Rappaport,

George R MacCartney, Shu Sun, and Shuai Nie. Millimeter-wave enhanced local area systems: A high-data-rate approach for future wireless networks. *IEEE Journal on Selected Areas in Communications*, 32(6):1152–1163, 2014.

[39] Marco Giordani, Marco Mezzavilla, C Nicolas Barati, Sundeep Rangan, and Michele Zorzi. Comparative analysis of initial access techniques in 5G mmwave cellular networks. In *Information Science and Systems (CISS), 2016 Annual Conference on*, pages 268–273. IEEE, 2016.

[40] Marco Giordani, Marco Mezzavilla, Sundeep Rangan, and Michele Zorzi. Multi-connectivity in 5g mmwave cellular networks. In *Ad Hoc Networking Workshop (Med-Hoc-Net), 2016 Mediterranean*, pages 1–7. IEEE, 2016.

[41] Marco Giordani, Marco Mezzavilla, and Michele Zorzi. Initial access in 5G mmwave cellular networks. *IEEE Communications Magazine*, 54(11):40–47, 2016.

[42] Felix Gutierrez, Shatam Agarwal, Kristen Parrish, and Theodore S Rappaport. On-chip integrated antenna structures in CMOS for 60 GHz WPAN systems. *IEEE Journal on Selected Areas in Communications*, 27(8), 2009.

[43] Shuangfeng Han, I Chih-Lin, Zhikun Xu, and Corbett Rowell. Large-scale antenna systems with hybrid analog and digital beamforming for millimeter wave 5G. *IEEE Communications Magazine*, 53(1):186–194, 2015.

[44] Steve Hilton. Machine-to-machine device connections: worldwide forecast 2010–2020. *Analysys Mason Report*, 2010.

[45] RJ Humpleman and PA Watson. Investigation of attenuation by rainfall at 60 GHz. In *Proceedings of the Institution of Electrical Engineers*, volume 125, pages 85–91. IET, 1978.

[46] Cheol Jeong, Jeongho Park, and Hyunkyu Yu. Random access in millimeter-wave beamforming cellular networks: issues and approaches. *IEEE Communications Magazine*, 53(1):180–185, 2015.

[47] Hamid Krim and Mats Viberg. Two decades of array signal processing research: the parametric approach. *IEEE signal processing magazine*, 13(4):67–94, 1996.

[48] Qian Clara Li, Huaning Niu, Geng Wu, and Rose Qingyang Hu. Anchor-booster based heterogeneous networks with mmwave capable booster cells. In *Globecom Workshops (GC Wkshps), 2013 IEEE*, pages 93–98. IEEE, 2013.

[49] Joseph C Liberti and Theodore S Rappaport. *Smart antennas for wireless communications: IS-95 and third generation CDMA applications.* Prentice Hall PTR, 1999.

[50] Duixian Liu and R Sirdeshmukh. A patch array antenna for 60 GHz package applications. In *Antennas and Propagation Society International Symposium, 2008. AP-S 2008. IEEE*, pages 1–4. IEEE, 2008.

[51] Jonathan S Lu, Daniel Steinbach, Patrick Cabrol, and Philip Pietraski. Modeling human blockers in millimeter wave radio links. *ZTE Communications*, 10(4):23–28, 2012.

[52] George R MacCartney and Theodore S Rappaport. 73 GHz millimeter wave propagation measurements for outdoor urban mobile and backhaul communications in New York City. In *Communications (ICC), 2014 IEEE International Conference on*, pages 4862–4867. IEEE, 2014.

[53] Andreas Maeder, Peter Rost, and Dirk Staehle. The challenge of M2M communications for the cellular radio access network. In *Proc. Würzburg Workshop IP, Joint ITG Euro-NF Workshop Vis. Future Gener. Netw. EuroView*, pages 1–2, 2011.

[54] Millimeter Wave As The Future Of 5G. Available: http://users.ece.utexas.edu/ rheath/presentations, 2015.

[55] Syed Ahsan Raza Naqvi and Syed Ali Hassan. Combining NOMA and mmWave Technology for Cellular Communication.

[56] Yong Niu, Yong Li, Depeng Jin, Li Su, and Athanasios V Vasilakos. A survey of millimeter wave communications (mmwave) for 5G: opportunities and challenges. *Wireless Networks*, 21(8):2657–2676, 2015.

[57] Muhammad Shahmeer Omar, Muhammad Ali Anjum, Syed Ali Hassan, Haris Pervaiz, and Qiang Niv. Performance analysis of hybrid 5G cellular networks exploiting mmwave capabilities in suburban areas. In *Communications (ICC), 2016 IEEE International Conference on*, pages 1–6. IEEE, 2016.

[58] Zhouyue Pi and Farooq Khan. An introduction to millimeter-wave mobile broadband systems. *IEEE Communications Magazine*, 49(6), 2011.

[59] Phil Pietraski, David Britz, Arnab Roy, Ravi Pragada, and Gregg Charlton. Millimeter wave and terahertz communications: Feasibility and challenges. *ZTE Communications*, 10(4):3–12, 2012.

[60] Jian Qiao, Xuemin Shen, Jon W Mark, and Yejun He. MAC-layer concurrent beamforming protocol for indoor millimeter-wave networks. *IEEE Transactions on Vehicular Technology*, 64(1):327–338, 2015.

[61] Zhao Qingling and Jin Li. Rain attenuation in millimeter wave ranges. In *Antennas, Propagation & EM Theory, 2006. ISAPE'06. 7th International Symposium on*, pages 1–4. IEEE, 2006.

[62] Vasanthan Raghavan, Juergen Cezanne, Sundar Subramanian, Ashwin Sampath, and Ozge Koymen. Beamforming tradeoffs for initial UE discovery in millimeter-wave MIMO systems. *IEEE Journal of Selected Topics in Signal Processing*, 10(3):543–559, 2016.

[63] Vasanthan Raghavan, Sundar Subramanian, Juergen Cezanne, and Ashwin Sampath. Directional beamforming for millimeter-wave mimo systems. In *Global Communications Conference (GLOBECOM), 2015 IEEE*, pages 1–7. IEEE, 2015.

[64] Sridhar Rajagopal, Shadi Abu-Surra, and Mehrzad Malmirchegini. Channel feasibility for outdoor non-line-of-sight mmwave mobile communication. In *Vehicular Technology Conference (VTC Fall), 2012 IEEE*, pages 1–6. IEEE, 2012.

[65] Theodore S Rappaport et al. *Wireless communications: principles and practice*, volume 2. Prentice Hall PTR New Jersey, 1996.

[66] Theodore S Rappaport, Felix Gutierrez, Eshar Ben-Dor, James N Murdock, Yijun Qiao, and Jonathan I Tamir. Broadband millimeter-wave propagation measurements and models using adaptive-beam antennas for outdoor urban cellular communications. *IEEE transactions on antennas and propagation*, 61(4):1850–1859, 2013.

[67] Theodore S Rappaport, Robert W Heath Jr, Robert C Daniels, and James N Murdock. *Millimeter wave wireless communications*. Pearson Education, 2014.

[68] Theodore S Rappaport, James N Murdock, and Felix Gutierrez. State of the art in 60-GHz integrated circuits and systems for wireless communications. *Proceedings of the IEEE*, 99(8):1390–1436, 2011.

[69] Theodore S Rappaport, Shu Sun, Rimma Mayzus, Hang Zhao, Yaniv Azar, Kevin Wang, George N Wong, Jocelyn K Schulz, Mathew Samimi, and Felix Gutierrez. Millimeter wave mobile communications for 5G cellular: It will work! *IEEE access*, 1:335–349, 2013.

[70] High Rate. GHz PHY, MAC and HDMI PAL, 2008.

[71] Syed Ahsan Raza, Syed Ali Hassan, Haris Bin Pervaiz, Qiang Ni, and Leila Musavian. Self-Adaptive Power Control Mechanism in D2D Enabled Hybrid Cellular Network with mmWave Small Cells: An Optimization Approach. 2016.

[72] John W Rittinghouse and James F Ransome. *Cloud computing: implementation, management, and security.* CRC press, 2016.

[73] Wonil Roh, Ji-Yun Seol, Jeongho Park, Byunghwan Lee, Jaekon Lee, Yungsoo Kim, Jaeweon Cho, Kyungwhoon Cheun, and Farshid Aryanfar. Millimeter-wave beamforming as an enabling technology for 5g cellular communications: theoretical feasibility and prototype results. *IEEE Communications Magazine*, 52(2):106–113, 2014.

[74] Richard Roy and Thomas Kailath. Esprit-estimation of signal parameters via rotational invariance techniques. *IEEE Transactions on acoustics, speech, and signal processing*, 37(7):984–995, 1989.

[75] Mathew Samimi, Kevin Wang, Yaniv Azar, George N Wong, Rimma Mayzus, Hang Zhao, Jocelyn K Schulz, Shu Sun, Felix Gutierrez, and Theodore S Rappaport. 28 GHz angle of arrival and angle of departure analysis for outdoor cellular communications using steerable beam antennas in New York City. In *Vehicular Technology Conference (VTC Spring), 2013 IEEE 77th*, pages 1–6. IEEE, 2013.

[76] Ralph Schmidt. Multiple emitter location and signal parameter estimation. *IEEE transactions on antennas and propagation*, 34(3):276–280, 1986.

[77] Stefania Sesia, Matthew Baker, and Issam Toufik. *LTE-the UMTS long term evolution: from theory to practice.* John Wiley & Sons, 2011.

[78] Sakir Sezer, Sandra Scott-Hayward, Pushpinder Kaur Chouhan, Barbara Fraser, David Lake, Jim Finnegan, Niel Viljoen, Marc Miller, and

Navneet Rao. Are we ready for SDN? Implementation challenges for software-defined networks. *IEEE Communications Magazine*, 51(7):36–43, 2013.

[79] Hossein Shokri-Ghadikolaei, Carlo Fischione, Gabor Fodor, Petar Popovski, and Michele Zorzi. Millimeter wave cellular networks: A MAC layer perspective. *IEEE Transactions on Communications*, 63(10):3437–3458, 2015.

[80] Hossein Shokri-Ghadikolaei, Lazaros Gkatzikis, and Carlo Fischione. Beam-searching and transmission scheduling in millimeter wave communications. In *Communications (ICC), 2015 IEEE International Conference on*, pages 1292–1297. IEEE, 2015.

[81] Sumit Singh, Raghuraman Mudumbai, and Upamanyu Madhow. Interference analysis for highly directional 60-GHz mesh networks: The case for rethinking medium access control. *IEEE/ACM Transactions on Networking (TON)*, 19(5):1513–1527, 2011.

[82] Sumit Singh, Federico Ziliotto, Upamanyu Madhow, E Belding, and Mark Rodwell. Blockage and directivity in 60 GHz wireless personal area networks: From cross-layer model to multihop mac design. *IEEE Journal on Selected Areas in Communications*, 27(8), 2009.

[83] Shu Sun, George R MacCartney, Mathew K Samimi, Shuai Nie, and Theodore S Rappaport. Millimeter wave multi-beam antenna combining for 5G cellular link improvement in New York City. In *Communications*

(ICC), 2014 IEEE International Conference on, pages 5468–5473. IEEE, 2014.

[84] Shu Sun, Theodore S Rappaport, Robert W Heath, Andrew Nix, and Sundeep Rangan. Mimo for millimeter-wave wireless communications: beamforming, spatial multiplexing, or both? *IEEE Communications Magazine*, 52(12):110–121, 2014.

[85] Y Ming Tsang, Ada SY Poon, and Sateesh Addepalli. Coding the beams: Improving beamforming training in mmwave communication system. In *Global Telecommunications Conference (GLOBECOM 2011), 2011 IEEE*, pages 1–6. IEEE, 2011.

[86] A Umer, S Hassan, H Pervaiz, Q Ni, and Leila Musavian. Coverage and rate analysis for massive mimo enabled heterogeneous networks with millimeter wave small cells. 2017.

[87] Vijay Venkateswaran and Alle-Jan van der Veen. Analog beamforming in MIMO communications with phase shift networks and online channel estimation. *IEEE Transactions on Signal Processing*, 58(8):4131–4143, 2010.

[88] EJ Violette, Richard H Espeland, and Gregory R Hand. Millimeter-wave urban and suburban propagation measurements using narrow and wide bandwidth channel probes. *NASA STI/Recon Technical Report N*, 86:25683, 1985.

[89] Junyi Wang. Beam codebook based beamforming protocol for multi-Gbps millimeter-wave WPAN systems. *IEEE Journal on Selected Areas in Communications*, 27(8), 2009.

[90] Damon Wischik, Mark Handley, and Marcelo Bagnulo Braun. The resource pooling principle. *ACM SIGCOMM Computer Communication Review*, 38(5):47–52, 2008.

[91] Feng Xia, Laurence T Yang, Lizhe Wang, and Alexey Vinel. Internet of things. *International Journal of Communication Systems*, 25(9):1101, 2012.

[92] Dipali S Yadav and Kanchan Doke. Mobile Cloud Computing Issues and Solution Framework. 2016.

[93] Hang Zhao, Rimma Mayzus, Shu Sun, Mathew Samimi, Jocelyn K Schulz, Yaniv Azar, Kevin Wang, George N Wong, Felix Gutierrez, and Theodore S Rappaport. 28 GHz millimeter wave cellular communication measurements for reflection and penetration loss in and around buildings in new york city. In *Communications (ICC), 2013 IEEE International Conference on*, pages 5163–5167. IEEE, 2013.

[94] Kan Zheng, Long Zhao, Jie Mei, Mischa Dohler, Wei Xiang, and Yuexing Peng. 10 gb/s hetsnets with millimeter-wave communications: access and networking-challenges and protocols. *IEEE Communications Magazine*, 53(1):222–231, 2015.

[95] Thomas Zwick, Troy J Beukema, and Haewoon Nam. Wideband channel sounder with measurements and model for the 60 GHz indoor radio

channel. *IEEE transactions on Vehicular technology*, 54(4):1266–1277, 2005.